POLITECNICO DI TORINO

MASTER's Degree in ELECTRICAL ENGINEERING

MASTER's Degree Thesis

Probabilistic Wind-Induced Failure Assessment of Double-Circuit Transmission Lines in High-Voltage Power Systems

Supervisors

Prof. Tao HUANG

Prof. Seyedmahmood HOSSEINIIMANI

Prof. Ettore Francesco BOMPARD

Candidate

Estefano DI GIACINTO

MARCH 2024

Probabilistic Analysis of EHV Double Circuits: Integrating VAFFEL Methodology and Markovian Chains

Estefano Di Giacinto

Abstract

The structural dependence of double-circuit transmission lines creates opportunities for CCF that can reduce capacity. To assess line vulnerability due to extreme wind stress, this work develops a dynamic simulator in place of static failure models. A multi-state Continuous Time Markov Chain (CTMC) model is developed and integrated with the VAFFEL methodology to simulate line performance as it transitions through degraded states of operation as well as during the simultaneous double circuit outage. Transition rates $\lambda(v_{wind})$ are dynamically calculated from site specific fragility functions.

ACKNOWLEDGMENTS

to my grandfather Mario

Table of Contents

List of Figures

List of Tables

Acronyms

TSO	Transmission System Operator.
RTN	Rete di Trasmissione Nazionale.
ROW	Right-of-Way.
CCF	Common Cause Failure.
MTTR	Mean Time To Repair.
MTTF	Mean Time To Failure.
CTMC	Continuous-Time Markov Chain.
Stochastic Race	The temporal competition during an extreme event between the failure rate of a redundant circuit and the restoration rate of the primary circuit already out of service.
Logistical Cliff	A critical threshold in MTTR beyond which the probability of system collapse increases non-linearly due to logistical delays or environmental constraints.
Reliability Gap	The discrepancy between normative reliability indices (based on average historical data) and the actual risk observed during localized extreme weather events.
Fragility Curve	A statistical function representing the probability of structural failure of a component (e.g., a transmission tower) as a function of an environmental load, such as wind speed.

Common Cause Failure	A single event that causes the simultaneous failure of multiple components that would otherwise be considered independent, often due to shared physical infrastructure.
Double-Circuit Line	A transmission line configuration where two independent three-phase circuits are supported by the same tower structure.

Chapter 1

Definition and Framework for Managing Double Circuit Lines

1.1 Introduction of Thesis Objectives

The increased reliability of double-circuit transmission lines can help TSOs address the challenge of increasing the capacity of a single right-of-way and improve the economic and land-use efficiencies of transmission. However, this also creates a structural dependency since the two circuits depend on the same towers, foundations, and environmental factors; therefore, the two circuits cannot be modeled independently of each other but instead must be evaluated as part of a unified multi-state system subject to common cause failures. When an extreme event occurs and causes the failure of a tower and/or the failure of a line due to high-velocity winds or a lightning strike, it is possible that there will be a simultaneous loss of both circuits which could act as a trigger for cascading failures across the regional network. This dissertation aims to reduce this vulnerability using a probabilistic risk assessment framework to replace deterministic planning approaches, such as the N-1 security criterion. This dissertation specifically investigates the degraded state of these corridors - the critical time interval where one circuit has failed while the other remains in operation. In addition to the conventional binary on/off reliability models used in most previous studies, this dissertation advances the VAFFEL methodology by implementing a 4-state continuous-time Markov chain framework which allows the determination of the persistence of the system under stressed conditions. A major contribution of this dissertation is the integration of different data sources. Through the use of Bayesian updating with empirical incident data from the Sicilian network, the model moves from uniform maintenance protocols to site-specific resilience strategies. It is recognized that the operational life cycle of infrastructure located in storm-prone corridors is fundamentally different than that of infrastructure located in protected environments. The organization of this dissertation follows a sequential format: after defining the initial framework, chapter 3 and 4 describes the methodological aspects of the dissertation, while chapter 5 presents the case study building scenario. Finally, chapter 6 evaluates the operational risk profiles, and the final chapter integrates the results of the dissertation and outlines potential avenues of research for improving grid resilience.

1.2 Regulatory Framework: Italy (Terna)

In the Italian energy sector, *Terna S.p.A.* acts as the Transmission System Operator (TSO), setting the technical and safety protocols for the National Transmission Grid (RTN) via the *Codice di Rete*. Within this regulatory framework, double-circuit infrastructures (*linee in doppia terna*) are classified as a strategic asset class. These assets are fundamental for ensuring compliance with the $N-1$ security mandate, particularly in high-capacity energy corridors [1, 2].

1.2.1 Technical Specifications

A double-circuit line is defined by Terna as an overhead, single tower structure supporting two independent, three-phase electrical systems. With the purpose of limiting the degree of electrical and mechanical interference, the technical configuration has been designed in accordance with strict geometric standards [3].

- Conductor Arrangements: The primary 380 kV circuits are implemented by Terna as triple-bundled (triplex) for reduction of the corona effect and improvement of thermal capability; whereas the 220 kV circuits are either twin-bundled (duplex) or single conductor [4, 5].
- Insulation and Lightning Safeguards: Standard 380 kV double-circuit towers employ glass or composite insulator strings, typically arranged in "I" or "V" patterns. To lower the probability of lightning-related Common Cause Failures (CCF), towers are fitted with one or two Optical Ground Wires (OPGW), which serve the dual purpose of providing lightning protection and facilitating high-speed data transmission [4].

1.2.2 Analysis of Strategic Case Studies

To evaluate the effectiveness of the stochastic reliability frameworks developed in this research, a set of key double-circuit infrastructures has been selected for detailed investigation. These specific grid assets were chosen because they exemplify the three fundamental dimensions of power system resilience: systemic redundancy, vulnerability to environmental stress, and the logistical challenges associated with restoration and recovery.

Table 1.1: Operational Parameters and Strategic Value of Selected Terna Double-Circuit Projects.

Infrastructure / Link	**Voltage**	**Configuration**	**Capacity (MVA)**
Sorgente - Rizziconi	380 kV	Hybrid AC Link	2000 per circ.
Bolano - Paradiso 2	380 kV	Submarine (2025)	1000 per circ.
Chiaramonte - Ciminna	380 kV	Overhead Triplex	3000 (Total)
Udine Ovest - Redipuglia	380 kV	Innovative Lattice	2500 (Total)
Piombino - Elba	132 kV	Submarine Cable	200 per circ.
Dolo - Camin	380 kV	Hybrid Section	2800 (Total)

The inclusion of these corridors in the study is predicated on their distinct functional and geographical profiles [6]:

- Sorgente-Rizziconi: As critical interconnections between Sicily and the Italian mainland, these links serve as primary models for investigating Common Cause Failures (CCF). They are essential for evaluating the transition from standard $N-1$ toward more robust $N-k$ security frameworks in high-priority transmission corridors.
- Chiaramonte-Ciminna: Acting as a vital line for the Sicilian interior, this line is frequently subjected to extreme Scirocco wind events. It provides a benchmark for modeling the probability of a secondary circuit failure occurring while the primary circuit is already undergoing repairs during prolonged weather disturbances.

1.2.3 Italy Protection: Dual-OPGW

In the Italian high-voltage context, Terna S.p.A. mandates a resilient communication architecture for strategic double-circuit lines. This framework is built upon the principle of path diversity to ensure the absolute reliability of high-speed protection schemes.

Selectivity of Protective Measures and Deterministic Communications

In order to ensure the reliability and stability of the electrical grid, Terna uses Current Differential Protection (87L) as its first line of defense in terms of unit protection; therefore, the operational effectiveness of this protection method is contingent upon the availability of a deterministic communication means. Typically, the deterministic communication means are provided by Optical Ground Wires (OPGW), as per reference [7].

- Path Redundancy and Diversification: With regard to the redundancy and diversity of paths on the 380 kV transmission lines, Terna has established a requirement that two independent OPGW paths be installed. As such, with the redundant paths in place, if the primary fiber path fails, the protection system will immediately switch over to the backup fiber optic path. If the failure of the primary fiber results in total isolation of both fiber optic paths, then the protection system will automatically transition into a fallback mode utilizing PLC-based Distance Protection (21).
- Latency and Jitter Requirements: As per Terna's Technical Specifications (Annex A.15) a maximum latency time of 5-10 ms is permitted for all fiber optic communication related to the operation of the protection systems so that there is sufficient time for the correct alignment of phasers prior to a protective relay tripping the circuit.

1.3 Regulatory Framework: Spain (Red Eléctrica)

Within the Spanish energy sector, the Transmission System Operator (TSO), *Red Eléctrica de España* (REE), establishes the engineering criteria for double-circuit infrastructures. These are defined as high-voltage transmission assets where a single structural support—typically a galvanized steel lattice tower—is designed to carry two autonomous three-phase electrical systems [8].

1.3.1 Technical Specifications

REE's technical specifications for the energy density of the energy infrastructure in these corridors have been developed as part of an effort to improve the resilience of the national grid. The following are the technical specifications that describe the design of these installations:

- Circuit autonomy and isolation: These circuits will be completely independent of each other electrically and mechanically. Each circuit will include its own unique conductor and insulating materials for the conductors so that if one circuit requires maintenance it can be done without affecting the operation of the second circuit.
- Advanced conductor topology: For the EHV 400 kV lines, REE requires the use of *bundle* configurations to maximize the heat transfer capability of the conductors. An example is the *Lada-Velilla* corridor, where REE uses ACSR (Aluminum Conductor Steel Reinforced) RAIL grade conductors in a triplex configuration to achieve a total heat transfer capacity of approximately 3210 MVA [9].

1.3.2 Analysis of Strategic Case Studies

The deployment of double-circuit technology across the REE network demonstrates its versatility in addressing diverse geographical and technical challenges, from inter-island links to high-capacity mainland lines:

Table 1.2: Landmark Double-Circuit Infrastructure Projects in the Spanish Power System.

Infrastructure Identifier	**Voltage**	**Engineering Features**
Lada - Velilla	400 kV	High-capacity EHV link utilizing triplex RAIL-type conductor bundles.
Abegondo - Mesón do Vento	400 kV	Critical Galician grid reinforcement employing duplex conductor technology.
Puente Bibey (Conso - Trives)	220 kV	Standard lattice tower deployment utilizing D4A4F support specifications.
Tenerife - La Gomera	66 kV	Deep-sea submarine interconnection reaching depths exceeding 1,100 meters.
Spain - Ceuta Link	132 kV	Strategic 58 km subsea double-circuit for inter-territorial supply security.
Rafal - Son Reus	220 kV	Hybrid transmission project combining overhead lattice and 2000 mm^2 underground sections.

1.3.3 Spain Protection (REE): Mutual Induction Paradigm

In the Spanish high-voltage network, *Red Eléctrica de España* (REE) implements a protection strategy specifically engineered to counteract the electromagnetic coupling characteristic of compact 400 kV double-circuit configurations [10].

Mutual Zero-Sequence Induction Compensation

The spatial proximity of parallel circuits in a double-circuit tower leads to significant mutual zero-sequence induction (Z_{m0}). During a single-phase-to-ground fault, the active circuit induces a zero-sequence voltage in the healthy parallel circuit. This phenomenon can cause numerical distance relays to misinterpret the fault location, resulting in selectivity issues such as overreaching or failing to trip (underreaching) [11].

- Vector 2 Utility: Diverging from the Italian backup-oriented model, the REE architecture utilizes the secondary communication vector for the real-time synchronization of zero-sequence current (I_0) phasors between the two parallel systems.
- Dynamic Impedance Correction: The protection IED (Intelligent Electronic Device) incorporates the current data from the adjacent line to dynamically adjust its impedance calculation via the following compensation logic: $V_{comp} = I \cdot Z_L + I_{0,parallel} \cdot Z_{m0}$[9, 4].

Teleprotection Redundancy and PLC Robustness

REE adopts a "Main 1 + Main 2" (M1+M2) redundancy philosophy, where both systems typically operate using Permissive Overreach Transfer Trip (POTT) logic to ensure instantaneous fault clearing across 100% of the line length [11].

- Phase-to-Phase PLC Coupling: To guarantee signal integrity during ground-fault conditions, REE mandates phase-to-phase coupling for its Power Line Carrier (PLC) systems [12]. This ensures that the high-frequency signaling can bypass a faulted conductor, maintaining communication continuity even when the OPGW path is compromised.

1.4 Regulatory Framework: France (RTE)

The French transmission system, managed by Réseau de Transport d'Électricité (RTE), constitutes one of the largest and most strategically central EHV networks in Europe. The technical governance of double-circuit lines (lignes à deux ternes) is dictated by the Schéma de Développement du Réseau (SDR), which enforces stringent $N-1$ security standards to ensure the stable evacuation of high-density power, primarily from the national nuclear fleet [13].

1.4.1 Structural Innovation and Geometric Standards

RTE's definition of a double-circuit line emphasizes the optimization of power density and the mitigation of environmental impacts. This is realized through advanced tower engineering and compact geometric configurations:

- Equilibre and Beaubourg Pylon Architectures: To minimize ground-level electromagnetic interference, RTE utilizes modern tower designs like the *Equilibre* and *Beaubourg*. The *Equilibre* tower, standing between 45–60 m, employs a vertical staggered phase arrangement. This geometry is designed to meet an ambitious magnetic field target of 0.4–3 μT in residential zones, significantly more restrictive than the statutory 100 μT limit [14].
- Conductor Bundling and Thermal Management: For the 400 kV corridors, RTE standardizes the use of *triple-bundled* (triplex) conductors with a 450 mm sub-conductor spacing. This increases the Surge Impedance Loading (SIL) to over 600 MW per circuit, enabling the management of massive nuclear power outputs that often exceed thermal ratings of 2500 MVA per circuit [4].

1.4.2 Technical Specifications

The expansion of the French double-circuit network is constrained by physical and regulatory thresholds:

- The 100 km AC Capacitive Threshold: RTE identifies a critical length of approximately 100 km for 400 kV AC double-circuits involving significant underground sections. Beyond this length, the reactive power generated by cable capacitance becomes difficult to compensate, frequently necessitating the adoption of HVDC technology for extended Alpine or subsea corridors [15].
- Mechanical Design and Reliability: In northern France, towers are engineered for extreme climatic loading (wind and ice), which directly dictates the structural failure rate (λ) utilized in the stochastic reliability models of this study.

1.4.3 Analysis of Strategic Case Studies

The following corridors have been selected as primary case studies due to their role in cross-border stability and their exposure to diverse failure modes.

Table 1.3: Strategic Double-Circuit Infrastructures and Resilience Parameters in the French Grid.

Infrastructure / Link	Voltage	Configuration	Strategic Resilience Factor
Avelin - Gavrelle	400 kV	Innovative "Equilibre" DT	Wind Resilience
Savoie - Piémont	320 kV	Hybrid HVDC Interconnection	Long-Distance Stability
Lonny - Vesle	400 kV	Overhead Double-Circuit	Benchmark for simulations
IFA-2 (France-UK)	320 kV	Submarine Double-Circuit	Critical Restoration Latency
Cotentin - Maine	400 kV	Strategic EPR Connection	N-k Contingency Management

These specific corridors highlight some of the multifaceted challenges of risk assestment in the French context:

- Avelin-Gavrelle: Utilizing the "Equilibre" structural design, this corridor is the benchmark for modeling failure rates in wind-prone northern regions.
- IFA-2: This subsea interconnection represents the ultimate model for critical restoration latency, where the extended repair time for submarine faults significantly increases the probability of a secondary contingency during the outage period [15].
- Cotentin-Maine - 400 kV The primary transmission route for evacuating Flamanville EPR (Third Generation Nuclear) power due to its high output capacity of 1650 MW. Any loss of both circuits of this line will have a significant impact as it has to be evacuated instantly into other parallel lines that are less strong than it. It could cause a cascade of N-k failures and instability throughout the entire western part of France's grid.

1.4.4 French Protection: Heterogeneous Strategy

To safeguard the 400 kV transmission grid, RTE implements a rigorous policy of "industrial diversity" for its double-circuit corridors. This strategy is specifically designed to eliminate Common-Mode Failures (CMF)—systemic vulnerabilities where a single software anomaly or manufacturing defect could simultaneously compromise both protection systems [14].

Multi-Vendor IED Architecture

RTE mandates a "Main 1 + Main 2" (M1+M2) architecture characterized by hardware and logical heterogeneity. This involves the deployment of two primary Intelligent Electronic Devices (IEDs) sourced from distinct manufacturers.

- System A (Primary - Main 1): This IED provides the primary Current Differential (87L) and distance (21) protection functions. It is interfaced with a dedicated OPGW fiber-optic pair to ensure high-speed, deterministic signaling [13].
- System B (Redundant - Main 2): To achieve industrial diversity, the second IED is sourced from an alternative vendor. It operates via a secondary, independent digital communication path to ensure total hardware and path segregation.
- Concurrent Operational Logic: Both systems operate in an active-active parallel configuration. This multi-vendor approach ensures that if one manufacturer's proprietary algorithm fails to recognize a complex fault signature, the diverse logic of the secondary terminal provides a fail-safe to clear the fault within the critical stability time [15].

1.5 Regulatory Framework: The German Quad-TSO

The German transmission architecture is characterized by a unique decentralized governance structure, managed by four distinct Transmission System Operators (TSOs): *Amprion, TenneT TSO, 50Hertz,* and *TransnetBW*. This collaborative framework is synchronized through the *Netzentwicklungsplan* (NEP) or Grid Development Plan, which aligns nationwide infrastructure expansion with the legal requirements of the VDE standards and the oversight of the Federal Network Agency (*Bundesnetzagentur*) [16].

1.5.1 Technical Specifications

Technical Specifications The main infrastructure in the German EHV network consists of double-circuit overhead transmission lines at the 380 kV and 220 kV voltage level. One of the typical characteristics of German grid construction is the Donau (Danube) tower structure which is an optimized version of a tower height in order to achieve adequate electrical separation between the two independent three-phase systems.

- Quad-Bundled Conductors (Viererbündel): The quad-bundled conductor configuration has become standard for 380 kV corridors. With four conductors per phase, it provides a substantial increase in the thermal capacity of the corridor, often enabling power transfers of over 3500 MVA; this allows the corridor to be less congested when peak renewable energy production occurs [17].
- Technological Transition to HVDC: As part of the national *Energiewende*, Germany is implementing the *SuedLink* project. This transition involves the deployment of High-Voltage Direct Current (HVDC) double-circuits primarily through underground XLPE cable systems. This shift from overhead to buried infrastructure introduces distinct technical restoration requirements and specialized maintenance protocols compared to traditional steel towers.

1.5.2 Strategic Infrastructure Case Studies

The German network incorporates several critical corridors that serve as primary references for analyzing grid reliability and structural failure modes (λ) within a high-density power system.

Table 1.4: Strategic Double-Circuit Case Studies in the German EHV Network.

Infrastructure / Link	Voltage	Technical Configuration	Capacity (MVA)
SuedLink (DC)	525 kV	Underground HVDC Double-Link	2000 per circ.
Wahle - Mecklar	380 kV	Quad-Bundled Overhead AC	3600 (Total)
Daxlanden - Eichstetten	380 kV	Strategic 380 kV EHV Corridor	2800 (Total)
Hansa PowerBridge	300 kV	Submarine Double-Circuit	700 per circ.
Bertikow - Pasewalk	380 kV	50Hertz Compact DT Design	2500 (Total)

These examples illustrate the diverse operational challenges facing the German grid:

- Wahle-Mecklar: As a vital North-South corridor, this link is the benchmark for modeling $N-1$ security thresholds. The high power density in this corridor necessitates advanced monitoring to prevent Common Cause Failures (CCF) on the parallel circuit during peak load periods.
- SuedLink: This underground EHV axis is a key model for analyzing restoration complexity. In contrast to the accessibility of overhead lines, faults in buried cable systems require specialized diagnostic equipment and significant civil engineering interventions, leading to recovery durations that are considerably longer than those of traditional overhead infrastructure [18].
- Hansa PowerBridge: A subsea interconnection with Scandinavia that faces unique recovery challenges related to maritime logistics and deep-water maintenance.

1.5.3 German Protection: Path Diversity

In the German EHV sector, Transmission System Operators (TSOs) such as Amprion and TenneT have transitioned toward integrated, high-availability communication frameworks. The current engineering philosophy prioritizes the encapsulation of protection signaling within deterministic wide-area networks (WAN), utilizing technologies such as Synchronous Digital Hierarchy (SDH) or Multiprotocol Label Switching - Transport Profile (MPLS-TP) [17].

Networked Protection and Deterministic Latency

The integration of protection data into a shared corporate grid infrastructure allows for enhanced path diversity and automated rerouting capabilities. This networked approach is designed to meet the rigorous timing requirements of EHV protection schemes:

- Primary Vector (Converged WAN): Protection signals are encapsulated within a deterministic network layer. This infrastructure provides sub-10 ms latency and sub-50 ms protection switching, ensuring that Current Differential (87L) phasors remain synchronized across the wide-area grid [16].
- Secondary Vector (Point-to-Point Optical Fiber): To maintain total signal independence, a secondary dark-fiber link is often deployed. This direct optical path ensures absolute reliability and serves as a non-networked backup to the primary digital vector.
- Tertiary Vector (PLC Tele-acceleration): For EHV corridors where fiber integrity might be compromised, German TSOs maintain legacy Power Line Carrier (PLC) systems. This channel provides a robust fallback for distance protection (21) tele-acceleration, ensuring fault clearance even in the event of a total optical failure.

1.6 Regulatory Framework: Norway (Statnett)

The Norwegian transmission system, operated by *Statnett SF*, provides a unique case study of extra-high-voltage (EHV) infrastructure engineered for extreme sub-arctic and maritime environments. The technical governance of double-circuit lines (*dobbelkurslinjer*) is centered on the requirement for high-capacity, resilient corridors to transport hydroelectric energy from remote production sites to urban load centers and international interconnectors [19].

1.6.1 Technical Specifications

Statnett's technical definition of a double-circuit line emphasizes mechanical over-design of the two circuits so as to ensure that they remain independent even when subjected to heavy weather conditions such as wet snow and icing. The engineering of these types of transmission lines includes certain characteristics of their structure:

- Tower Design and OPGW Shielding: Reinforced lattice masts or modern Y-towers are used by Statnett for the 420 kV double-circuit lines. The tower designs include a small shielding angle ($< 20°$) for the dual Optical Ground Wires (OPGW) and are thus capable of preventing lightning strikes on the phase conductors in mountainous areas.

- Ice and Wet Snow Loading: Double-circuit designs made in Norway have been designed to support extreme amounts of "wet snow" and ice. Towers and hardware for conductors in high altitude or coastal transmission routes are built to withstand accumulations of up to 30 kg/m of ice, this amount is greater than typical European design limits [20].

- Bundle Configuration to Prevent Conductor Galloping: Bundled conductors are used by Statnett to allow for high power density while ensuring the aerodynamic stability of the bundles. The bundles are typically duplex or triplex, and are spaced further apart than sub-conductors to reduce the likelihood of "galloping" and mechanical interaction between the two independent circuits at high velocity winds.

1.6.2 Analysis of Strategic Case Studies

The Norwegian network incorporates several strategic double-circuit corridors that provide the primary data for modeling failure rates (λ) and recovery durations (μ) in high-impact environments.

Table 1.5: Strategic Double-Circuit Case Studies within the Statnett EHV Grid.

Infrastructure / Link	Voltage	Technical Configuration	Capacity (MVA)
North Sea Link (NSL)	515 kV	Submarine Double-Link (DC)	1400 (Total)
Ofoten - Balsfjord	420 kV	Overhead Arctic Double-Circuit	2500 (Total)
Ørskog - Sogndal	420 kV	Mountainous EHV Line	2800 (Total)
NordLink (NO - DE)	525 kV	Submarine Double-Circuit	1400 (Total)
Lyse - Stølaheia	420 kV	High-Capacity EHV Corridor	2100 per circ.

These specific infrastructures represent the boundary conditions for the stochastic reliability models proposed in this thesis:

- Ofoten-Balsfjord: Situated above the Arctic Circle, this 420 kV double-circuit line is the benchmark for structural survival. The probability of failure (λ) is modeled against prolonged icing and wind-loading events that test the mechanical limits of the tower-conductor interface.
- North Sea Link & NordLink: These submarine interconnections represent the ultimate case studies for recovery durations. Due to the maritime logistics and deep-sea technical challenges involved, the mean time to repair (μ) for these submarine double-circuits is significantly higher than that of overhead alternatives, particularly during winter storm seasons [21].

1.6.3 Norway Protection (Statnett): Reinforced Infrastructure

The Norwegian Transmission System Operator, *Statnett*, operates in a sub-arctic climatic environment that imposes extreme mechanical stress on grid infrastructure. Consequently, the protection philosophy for 420 kV double-circuit lines prioritize the structural durability of communication vectors against intense ice accretion and high-velocity wind events. To mitigate the risk of concurrent mechanical failure, Statnett frequently deploys redundant OPGW systems with differentiated physical characteristics [20].

Mechanically Reinforced Optical Infrastructure

To ensure the absolute reliability of the 420 kV corridors, Statnett utilizes a hierarchical communication strategy based on environmental hardening and path diversity:

- High-Tensile OPGW (Dark Gray): These are mechanically reinforced fiber-optic cables specifically engineered to withstand extreme ice loading. This vector serves as the primary medium for the synchronization of Current Differential (87L) phasors [21].
- Redundant Optical Path (Violet): A secondary fiber-optic route is established to provide path diversity. This link is typically integrated into a separate shield wire or utilizes a diverse geographical entry point near substations to ensure that a localized mechanical disturbance does not compromise both communication channels.
- Autonomous Path Restoration: Given the remote nature of Nordic terminal nodes, Statnett emphasizes "Self-Healing" protection logic. The protection IEDs (Intelligent Electronic Devices) are capable of instantaneous failover between OPGW paths without losing phasor synchronization, maintaining a deterministic latency of less than 10 ms even during severe winter disturbances [19].

1.7 Regulatory Framework: Switzerland (Swissgrid)

The Swiss transmission system, operated by *Swissgrid*, functions as the central "Electricity Turntable" of Europe, facilitating critical North-South energy transits across the Alpine massif. Due to Switzerland's restrictive environmental regulations and challenging topography, Swissgrid's engineering philosophy for double-circuit lines is characterized by the Hybrid Corridor concept—a systemic integration of overhead and underground transmission technologies [22].

1.7.1 Mixed-Media Transmission

Switzerland is one of the world leaders in the partial cabling (undergrounding) of double-circuits for transmission at 380 kV EHV. The architectural choice of mixed-media transmission creates specific technical discontinuities:

- Transition Stations as Interfacial Nodes: Swissgrid has to manage transition points in the form of transition stations between overhead line towers and high-voltage XLPE (cross-linked polyethylene) cable systems, which are part of underground grid sections. The transition stations are considered reliability-critical nodes, since the transition from the climate-related failures of the overhead lines to the thermal and dielectric stressors of the underground cables create a new class of failure intensity λ[23].
- Compact Tower Geometry in Narrow Alpine Valleys: In order to minimize both the visual and electromagnetic footprint in narrow alpine valleys, Swissgrid often employs compact tower designs (for example the "Pylone T" or steel pole structures), which significantly reduces the ROW and the ground level magnetic fields generated by the transmission lines. However, the compact design also reduces the clearances between phases and circuits on the compact towers. As a result, Swissgrid has to employ more stringent insulation coordination than before in order to mitigate the increased risk of CCF (common cause failures) caused by atmospheric surges.

1.7.2 Analysis of Strategic Case Studies

The following case studies illustrate the application of Swissgrid's hybrid and compact design philosophies in diverse geographical contexts.

Table 1.6: Landmark Double-Circuit Infrastructures in the Swiss EHV Network.

Infrastructure / Link	Voltage	Technical Profile	Operational Status
Beznau - Birr	380 kV	Hybrid (Overhead-Underground)	Operational
Chamoson - Chippis	380 kV	High-Capacity Alpine Corridors	Operational
Gösgen - Mühleberg	380 kV	Strategic East-West Intertie	Active Upgrade
Niederwil - Obfelden	380 kV	Multi-Circuit Compact Corridor	Planning Stage

1.7.3 Switerzaland Protection (Swissgrid): Microwave Strategy

In the high-altitude regions of the Swiss Alps, *Swissgrid* operates under severe environmental constraints, where phenomena such as conductor galloping and avalanche-induced tower displacement pose a continuous threat to structural integrity. To ensure the reliability of the 380 kV corridors, Swissgrid adopts a philosophy of Topographical Path Diversity, utilizing a non-contact terrestrial microwave backhaul to maintain protection continuity even in the event of total mechanical destruction of the transmission line [23].

Structural Decoupling

The Swissgrid communication structure was developed to separate the protection signaling process from the actual state of the electric power corridor.

This separation of the protection signaling process from the physical status of the electric power corridor can be achieved by the use of two entirely different media of propagation:

- Vector 1 (Alpine OPGW): The main communication channel is formed by a high-bandwidth optical fiber core that is embedded in the tower's shield wire. This link will support the deterministic synchronization that is needed for current-differential (87L) protection systems [22].
- Vector 2 (Line-of-Sight Microwave Backhaul): For the purpose of providing a fail-safe should the mechanical structure of the electric power corridor fail due to an avalanche, Swissgrid has developed an extensive point-to-point microwave communication network that operates on frequencies between 7 GHz and 38 GHz. As the microwave link is positioned completely outside of the transmission towers, its geographic position cannot be affected by a structural failure in the transmission towers, which provides assurance that an avalanche or structural failure in the transmission towers will not affect the secondary communication channel.
- Transition and Failover Logic: The protection IEDs (Intelligent Electronic Devices) are continuously monitoring the quality of the optical signals that are being transmitted over the optical link. In the case of a rupture of the optical link, the system automatically transitions to the microwave backhaul as a means of fail-over. Although the wireless link will cause some slight degradation in jitter, it will still meet all of the requirements for the acceleration of time-distance protection (21) and the backup synchronization of differential protection [24].

1.8 Regulatory Framework: United Kingdom (National Grid)

The U.K.'s transmission system is managed by National Grid Electricity Transmission (NGET). The NGET transmission system is located in a marine climate with variable conditions which necessitates a technical approach to manage the structural vulnerability of the double-circuit infrastructures particularly within high salinity coastal corridors and wind prone areas [25].

1.8.1 Structural Innovation: The T-Pylon Monopole

There has been a major transformation of the U.K.'s grid structure since the introduction of the T-Pylon, an innovative monopole design for 400 kV double circuit lines. This represents a fundamental departure from the traditional lattice tower design:

- Rhomboidal Insulator Geometry: The T-Pylon employs a rhombus-shaped (diamond-shaped) insulator configuration. This geometric shape has been developed to minimize the impact of wind induced oscillations and conductor vibration.
- Visual and Environmental Mitigation: By decreasing the height of the monopoles as well as the quantity of structural elements, the T-Pylon significantly reduces the ROW footprint of the infrastructure while providing the same level of mechanical resiliency needed for dense 400 kV EHV transmission [26].

1.8.2 Offshore Integration

The Offshore Transmission Network Review (OTNR) of the U.K. represents a major transition in the grid architecture from isolated "links" for renewable energy evacuation to "hubs". This architectural shift will require increased reliability standards:

- Systemic Accumulation of Risk: As described above, multi-circuit offshore hubs represent a high density of risk. A single structural failure or localized disruption on a coastal double circuit tower could result in the immediate de-energizing of multiple gigawatts of offshore wind generation thus requiring $N - k$ contingency planning at the system level.
- Recovery Time Frames and Accessibility: Similar to the Nordic interconnections, for offshore or coastal double circuits, the time frame for restoration is very much contingent upon maritime accessibility. Repair operations for these structures may be limited to weather windows and/or availability of vessels that are capable of accessing the zone where the repair is to be performed [27].

Table 1.7: Landmark Double-Circuit Infrastructures in the UK National Grid.

Infrastructure / Link	Voltage	Technical Profile
Hinkley Connection	400 kV	Inaugural T-Pylon Corridor
Viking Link	525 kV	Submarine Double-Link (HVDC)
Bramford - Twinstead	400 kV	Strategic Regional EHV Reinforcement
Western Link	600 kV	Subsea HVDC Double-Circuit

The Hinkley Connection provides the empirical baseline for analyzing the failure rate of the T-Pylon under maritime wind stress. Concurrently, theViking Link serves as a critical model for analyzing extended restoration intervals, where the time-to-recovery is influenced by the stochastic nature of North Sea maritime logistics.

1.8.3 UK Protection (NGET): Intertripping

In the high-density EHV corridors of the United Kingdom, *National Grid Electricity Transmission* (NGET) prioritizes a communication architecture optimized for high-speed intertripping and Direct Transfer Trip (DTT) functionality. This strategy is centered on the utilization of a dedicated, private fiber-optic infrastructure to maintain absolute control over propagation latency and signal jitter, ensuring the stability of the 400 kV double-circuit grid [26].

Path Segregation and Signaling Prioritization

NGET's protection philosophy mandates a hierarchical communication framework where protection signaling is prioritized over all other data traffic to meet stringent fault-clearing time requirements:

- Dedicated Intertripping Network (Red): This vector represents a private wide-area fiber network reserved for high-speed Direct Transfer Trip (DTT) signaling. This infrastructure ensures that a fault detected at a local substation can trigger the instantaneous opening of remote circuit breakers across the corridor, effectively neutralizing the fault within milliseconds [27].
- High-Speed Protection Interface (Orange): A secondary, point-to-point optical link is established between Intelligent Electronic Devices (IEDs) for the real-time exchange of current phasors. This vector supports the synchronous differential logic (87L) required for the $N-1$ security of the double-circuit line.
- Hierarchical Confirmation Logic: To enhance system safety and prevent maloperation, NGET incorporates interlocking logic within the communication protocol. This requires the protection terminal to confirm the fault status from the remote end via the segregated communication path before executing a final trip command, ensuring 100% selectivity [25].

Chapter 2

TSOs Practices for Contingency Analysis

2.1 Regulatory Framework: ENTSO-E and ACER Classifications

The management of double-circuit failures within the European Internal Energy Market is governed by a rigorous regulatory hierarchy, established primarily by the System Operation Guideline (SOGL) [28] and further operationalized through the Coordinated Security Analysis Methodology (CSAM) [29]. These frameworks provide the standardized taxonomy required for cross-border security, distinguishing between ordinary, exceptional, and out-of-range contingencies based on their statistical probability and potential for systemic instability.

2.1.1 Categorization of Double-Circuit Faults

As specified in Article 33 of the SOGL [28], the simultaneous trip of two or more circuits sharing a common support structure is formally classified as an *exceptional contingency*. In traditional deterministic planning, such events were often excluded from the active N-1 security list due to their low historical frequency. This exclusion is a necessary compromise for market efficiency; requiring constant N-2 security for every shared corridor would lead to permanent grid congestion and prohibitive redispatch costs.

However, recent amendments by the Agency for the Cooperation of Energy Regulators [30] have redefined this boundary. The current regulatory trend moves away from a static, binary classification of credible versus non-credible events, favoring a conditional approach that acknowledges the physics of the asset under environmental stress.

2.1.2 Occurrence Increasing Factors (OIF)

The second amendment to the CSAM [30] introduces the technical concept of Occurrence Increasing Factors (OIF). These represent specific conditions that mandate a TSO to elevate an "exceptional" event to the "credible" list. These factors are divided into two distinct categories:

1. Permanent OIF: These relate to the inherent structural or geographical vulnerability of the asset. This includes older lattice tower designs with limited mechanical redundancy or lines situated in terrain prone to geological displacement.

2. Temporary OIF: These are dynamic, time-limited triggers that escalate failure probability. The methodology explicitly identifies extreme weather—such as wind gusts approaching the mechanical design limits defined in *CEI EN 50341-1* [31]—as well as icing, lightning, or localized equipment malfunctions.

2.1.3 Dynamic Transition to Operational Credibility

Under this revised methodology, the operational status of an exceptional contingency is no longer fixed; instead it can be dynamically changed when there is an active temporary outage (TOF) in place. Once there is a TOF in place, the Transmission System Operator

(TSO) is legally required to recategorize a simultaneous loss of the two circuits in the double-circuit corridor as credible in terms of risk. In most cases, this change in status will occur when meteorologic forecasts show that the loads on the environment are approaching the structural limit of the structures.

When a contingency is considered credible, it triggers a mandatory coordinated security assessment, usually managed at the regional level by RCCs (Regional Coordination Centers), and the TSO is required to identify the necessary corrective/preventative remedial action(s), including generation redispatch or pre-emptive topology adjustments. The purpose of these actions is to ensure that the system continues to operate within acceptable limits even if the shared corridor loses both of its circuits, thereby avoiding localized structural failures from spreading to become large-scale cascading blackouts across the entire interconnected European grid. This legal requirement directly motivates assessing structural vulnerability as a dynamic factor in determining the reliability of a power system.

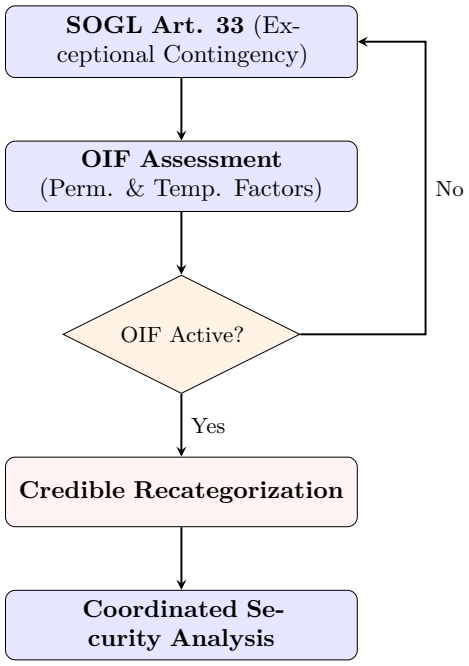

Figure 2.1: Regulatory contingency recategorization process.

2.2 Terna S.p.A.: Management of Double-Circuit Infrastructure

In the Italian regulatory framework, Terna S.p.A. integrates the management of double-circuit failures into its broader "Resilience Methodology," formally codified as Allegato A76 to the Grid Code [32]. Terna identifies double-circuit outages as common-mode failures (*guasti di modo comune*), where the physical proximity of conductors on a single support structure transforms a single structural fault into a simultaneous loss of two circuits [33, 32].

2.2.1 Common-Mode Contingency Modeling

While standard grid security relies on the deterministic N-1 criterion, Terna treats the simultaneous outage of both circuits on a shared structure as a specific type of contingency in its simulations:

- Contingency Classification: Contemporaneous outages of double-circuit lines at 380-220 kV, or 150-132 kV within an operating island, are formally considered N-1 contingencies if they have the potential to cause significant current redistribution [33].
- Probabilistic Shift: Beyond deterministic snapshots, Terna utilizes probabilistic simulations to weigh these N-k events based on their probability of occurrence, moving beyond fixed failure rates to dynamic vulnerability assessments [33].

2.2.2 Environmental Stressors and Fragility

Terna's methodology identifies specific extreme weather phenomena that trigger common-mode failures by overwhelming the mechanical capacity of shared towers [34, 32, 35]:

- Wet Snow Sleeves (*Manicotti di neve umida*): The accretion of wet snow adds critical weight to conductors and guard wires, leading to simultaneous short circuits or structural tower collapse [34, 32, 35].
- Strong Winds: Beyond direct structural stress, high wind speeds frequently cause the falling of nearby vegetation onto conductors, which Terna identifies as a primary cause of double-circuit service interruptions [32, 35].
- Salt Contamination: During prolonged droughts, saline deposits accumulate on insulators; subsequent moisture can trigger simultaneous surface discharges across both circuits [34, 32, 35].
- Hydrogeological Instability: Floods and landslides are explicitly modeled as drivers for foundation failure, resulting in the total collapse of shared towers [34, 32, 35].

2.3 Red Eléctrica de España (REE): Management of Double-Circuit Infrastructure

In the Spanish regulatory framework, Red Eléctrica de España (REE), acting as the Transmission System Operator (TSO), manages grid security and double-circuit contingencies through the *"Procedimientos de operación"* (Operating Procedures), specifically P.O. 1.1 [36, 37]. REE identifies these events as specific contingencies that must be accounted for in both operational planning and real-time management to guarantee supply continuity [36].

2.3.1 Double-Circuit Contingency Modeling

While the Spanish grid typically operates under the deterministic N-1 criterion—defined as the simple failure of any single system element such as a generator, line, transformer, or reactor—specific technical thresholds are defined for double-circuit lines [36, 38]:

- Contingency Classification: REE formally considers the simultaneous failure of both circuits on a double-circuit line as a contingency if they share support structures for more than 30 kilometers of their route [36]. For lines constructed or renewed after the year 2005, this distance threshold is extended to 50 kilometers [36].
- Security Thresholds: Following a double-circuit loss, the system must remain stable without resulting in market curtailments [36]. Admissible voltage limits for a 400 kV network during these events are widened to a range of 375 kV to 435 kV (compared to the standard 380-435 kV for N-1 events) [36].
- Prevention of Voltage Collapse: Beyond fixed limits, REE is mandated to ensure that no condition of voltage instability exists that could lead to a total grid collapse [36].

2.3.2 Systemic Stressors and Vulnerability

Recent analysis identifies several systemic stressors that increase the risk of contingencies and complicate the management of Spain's 45,500 km of circuits [37, 38]:

- High Renewable Penetration: The growth of non-synchronous renewable generation (solar PV and wind) has introduced a lack of dynamic voltage regulation capacity, as these installations traditionally operate under a fixed power factor in Spain [38].
- Low Synchronous Generation: A decrease in the energy mix of "conventional" or synchronous generation (nuclear, CCGT, hydro) reduces the system's ability to absorb reactive power, leading to severe overvoltage fluctuations that can trigger protective disconnections [38].
- Interconnection Variability: High variability in exchanges with Portugal and France—including abrupt reversals in power flows—introduces fluctuations in reactive power that stress the transmission grid's voltage profile [38].

- Environmental Management: REE identifies vegetation management and fire prevention as critical sustainability pillars for protecting high-voltage infrastructure integrated into the territory [37].

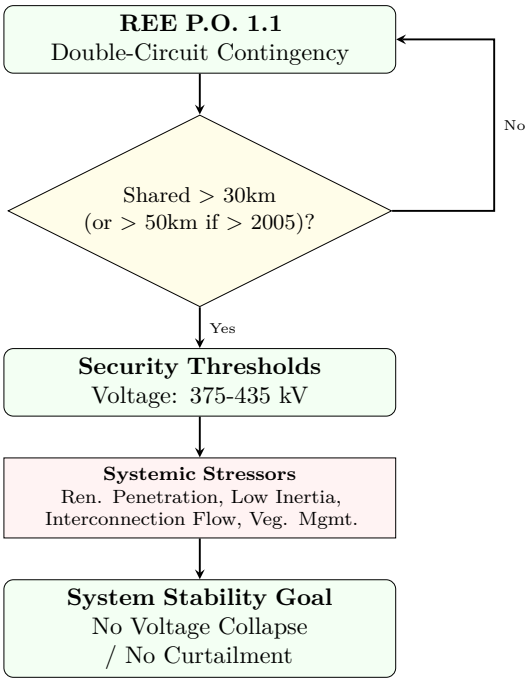

Figure 2.2: REE Operating Procedure P.O. 1.1: Double-circuit contingency assessment and stressor management.

2.4 Réseau de Transport d'Électricité (RTE): Management of Double-Circuit Infrastructure

In the French regulatory framework, Réseau de Transport d'Électricité (RTE) manages the operational safety of its 400 kV and 225 kV double-circuit infrastructure under Article 28 of the public transmission system grid-concession specifications [39]. RTE defines system safety as the ability to control system reactions to hazards—specifically the unexpected unavailability of transmission installations—to ensure frequency, voltage, and intensity remain within operating ranges considered to be risk-free [39].

2.4.1 Double-Circuit Contingency Modeling

While nominal grid operation follows a standard deterministic security principle, RTE's safety framework distinguishes between standard contingencies and the more severe common-mode risks posed by shared-support infrastructure [39, 40]:

- Contingency Categorization: RTE distinguishes between Standard Hazard Conditions (*Aléas courants*), which include nominal N-1 contingencies where normal operation must be maintained, and Adverse Hazard Conditions (*Aléas défavorables*), which encompass more severe incidents such as the simultaneous failure of both circuits on a shared tower [39]. For these adverse events, the goal shifts from maintaining normal ranges to minimizing the number of incidents and preventing their escalation into major system failures [39].

- Significant System Events (SSE): The grid's performance is monitored through an event classification with severity ranking of 0 to F [39]. When accepted risk levels (standard N-1 safety margins) have been breached for temporary periods, they can be classified as Level-B SSEs. In 2024, RTE reported that there had been an extremely high number of these events, in comparison to 2023 (23 vs. 3). These events were categorized as "complex conditions," which resulted in the system being exposed to increased vulnerability for approximately 40 hours on average, particularly at the border areas of Italy and Switzerland [39].

- Automated Defense Schemes: Because electrotechnical phenomena from adverse hazards can develop too rapidly for human intervention, RTE employs automated regional schemes [39]. These include the Western Automatic Scheme against Voltage Collapse (ADO) and the Northern Automatic Scheme (ADN), designed to trigger localized load-shedding to prevent regional voltage collapse following a simultaneous corridor trip [39].

2.4.2 Systemic Stressors and Vulnerability

Latest prospective studies identify several systemic and environmental stressors that escalate the probability of common-mode failures and complicate real-time contingency management [40, 41, 42]:

- Thermal Stress and Conductor Sag: Extreme heat causes cables to expand and elongate, potentially breaching safety distances and leading to simultaneous phase-to-ground faults [39, 41]. To mitigate this, future 400 kV lines are designed for an 85°C distribution temperature (an increase from 65°C) to maintain safety margins during a projected +4°C climate trajectory [41].
- Structural Doubling and Redundancy: To physically de-risk the loss of corridors in high-consumption industrial hubs like Dunkerque, Le Havre, and Fos, RTE is doubling segments of the 400 kV network to accommodate massive new consumption requests ranging from 250 MW to 750 MW per project [40, 41].
- Cross-Zonal Transit Flows: As a central hub for European power, France is exposed to "cross-zonal transit flows" originating in distant regions (e.g., from Spain to Germany) [39]. These flows often bring interconnection loads close to operating limits, reducing the available margin to absorb the loss of a double-circuit line [39].
- Environmental and Hydrogeological Risks: RTE models risks from major storms, maintaining a securing program for wind speeds of 180 km/h, and manages substations in flood-prone areas, which currently include 18% of the 400 kV sites [40, 41].

2.5 German TSOs: Management of Double-Circuit Infrastructure

In Germany, the security of the transmission grid is governed by the latest VDE application rules, specifically VDE-AR-N 4130 (TAR Extra-High Voltage), which defines connection requirements for the extra-high voltage grid ($\geq$ 220 kV) [43]. The German TSOs (Amprion, TenneT, 50Hertz, and TransnetBW) manage double-circuit corridors as critical infrastructure under the NOVA principle—prioritizing grid optimization and reinforcement before expansion—a framework formally integrated into the 2037/2045 Network Development Plan (NEP) [44, 45]. This planning ensures that nationally uniform requirements are implemented to maintain system stability in compliance with European law [46, 43].

2.5.1 The Extended (n-1) Criterion and Curative Measures

The German methodology is defined by the application of the extended (n-1) criterion (erweitertes (n-1)-Kriterium) [45]. This standard ensures that the grid remains stable even if a contingency occurs while another element is already out of service for planned maintenance [45].

- Curative System Operation: To mitigate the impact of double-circuit outages and reduce preventive costs, TSOs are moving toward curative system operation [44]. This utilizes congestion management (Engpassmanagement) to adjust power plant outputs or flexible loads to maintain the grid within safe limits [45].
- Innovative Remedial Actions: To protect the 380 kV lines, Germany is deploying *"Netzboosters"* (large-scale battery storage) and automated remedial schemes [44]. These allow for millisecond-responses to manage contingencies, enabling higher utilization of the existing shared-tower infrastructure [44, 45].

2.5.2 System Stressors and Infrastructure Vulnerability

German methodology identifies the rapid transformation of the energy system as a primary stressor, where the increasing number of decentralized renewable plants makes supply management significantly more complex than with conventional large-scale plants [46, 43]. TSOs must manage specific vulnerabilities arising from the decoupling of generation and load:

- Loss of System Inertia: The decommissioning of nuclear and coal-fired power plants has led to a critical reduction in rotating masses [44]. This loss of inertia increases the grid's vulnerability to frequency disturbances, requiring TSOs to implement innovative tools like rotating phase shifters and grid-forming converters to provide the necessary momentary reserve [45, 44].
- Structural Congestion and Shared Towers: As Generation has shifted to the northwest part of Germany, this causes structural congestion issues with transporting that electricity from the generators to industrial centers in the west and south [44, 45]. Additionally, the structural vulnerability of shared tower corridors (hybrid towers that carry both AC and DC) are increased due to the fact that one mechanical failure or lightning strike on either circuit can cause a large scale common mode outage [44, 45].
- Climatic Thermal Stress: Real-time environmental factors such as high ambient temperatures and low wind speeds act as stressors by limiting the thermal capacity of overhead lines [45, 44]. To manage this, TSOs utilize weather-related overhead line operation (WAFB) under VDE-AR-N 4210-5 to adapt transmission capacity to environmental conditions and prevent regional voltage collapse during high-load periods [47, 44].

2.6 The roadmap for unifying practice

The methodology for ensuring the reliability of the European high-voltage transmission grid has undergone a profound transformation, evolving from rigid deterministic rules to dynamic, probabilistic frameworks.

2.6.1 European Power Systems Prior to the 1990s

Prior to the 1990s, the reliability of European power systems were based upon deterministic N-1 criteria for power system operational safety. This is an expectation that the power system should be able to operate safely under the loss of any one component of the power system at any time. The reliability management of power systems prior to the 1990s have historically been performed through several unstandardized fault recording systems, many of which serve no standardized purpose for each voltage level. For example, the Norwegian System Operator, Statnett used the SDI system to support disturbance management until the entire power sector became nationalized and the entire country was required to follow a national standard.

2.6.2 Standardizing Reliability Data Collection in Norway: FASIT (1990-1995)

The development of data-based reliability began in Norway with the enactment of the Energy Act in 1990, which added additional requirements for the reporting of quality of supply and interruption. The creation of FASIT (Fault and Interruption Statistics in the Total Grid) was created in 1993 in response to this new legislation. FASIT was designed to provide a centralized framework for collecting reliability statistics and analyzing those results [48]. After successfully completing a test phase in 1994, FASIT was fully implemented nationally in 1995. The implementation included mandatory forms and procedures for collection of reliability data at all voltage levels. As such, FASIT eliminated the need for disparate fault tracking systems in place prior to the establishment of the FASIT database and provided a unified international source for the most recent reliability data for over 30 years.

2.6.3 Probabilistic Reliability Framework Development in Europe: GARPUR (2013 – 2017)

As the complexity of power grids increased due to the incorporation of renewable energy into existing power systems, the European GARPUR project was initiated in 2013 to develop the next generation of reliability models for the pan-European level [49]. GARPUR produced the Reliability Management Approach and Criterion (RMAC). The RMAC produced a method to move from worst case to probabilistically analyze the likelihood of a failure occurring and the socio-economic consequences associated with the failure. The research demonstrated that reliability can be managed using a probabilistic approach to achieve a balance between reliability expenditure and reliability of service.

2.6.4 Development of the VAFFEL Engine (2016–Present)

During this same period, technical work on calculating dynamic risk metrics intensified. In 2016, researchers from Statnett and SINTEF published the methodology for wind-dependent failure rates using a Bayesian updating scheme [50]. This research forms the core of the VAFFEL engine (*Varsel Før Feil*), which adjusts global failure rates with individual historical data from systems like FASIT to establish "fragility curves" for specific line segments. By combining these curves with real-time weather reanalysis data, VAFFEL provides a means to calculate hourly probabilities of failure.

2.6.5 The Road to 2027: The ENTSO-E Mandate

In 2019, an ACER decision established the legal mandate for all European TSOs to move toward Probabilistic Risk Assessment (PRA). Currently, ENTSO-E is executing a roadmap to develop a common European PRA methodology by December 2027 [51]. As part of this roadmap, the VAFFEL engine is identified as a primary candidate for probability calculations. The first large-scale tests of the VAFFEL computations on the PRA dataset were scheduled to launch in early 2024, representing the final stage in the transition from static deterministic rules to a dynamic, risk-based operational system.

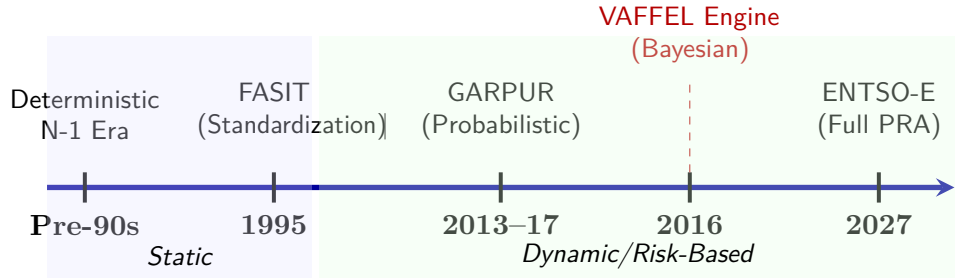

Figure 2.3: Timeline of the evolutionary shift in European grid reliability methodologies.

2.7 Summary

This chapter has provided a critical review of the evolving landscape of contingency analysis practices adopted by Transmission System Operators (TSOs) across Europe. The analysis reveals a significant paradigm shift from the traditional, deterministic $N-1$ security criteria—which served as the cornerstone of grid operation for decades—toward more sophisticated, risk-based probabilistic frameworks.

The shift toward integrated reliability models (as proposed through international initiatives such as GARPUR and ENTSO-E) from traditional structural assessments necessitates consideration of the probabilistic nature of environmental stressors. By assessing the operational strategies of the major European Transmission System Operators (TSOs), i.e., Terna, REE, and RTE; it becomes apparent that the operational management of double-circuit lines can only be accomplished with a detailed understanding of both common-mode failures and the temporal intensification of failures that static contingency listings cannot provide.

Ultimately, the inadequacies of current deterministic-based approaches identify a critical need for the development of dynamic, state-space representations. The inability of current operational standards to accurately describe the time-varying evolution of lines health due to storms identifies the primary driving force behind the next chapters, where we propose to address the gap identified here through the introduction of a comprehensive Markovian reliability model that transforms static fragility assessments into a time-dependent operational risk profile that can be used to inform modern grid-hardening practices.

TSO / Entity	**Core Strategy**	**Contingency Focus**	**Key Innovation**
Terna (SOGL)	Exceptional to Credible	Dynamic OIF factors	Dynamic Risk Assessment
REE (P.O. 1.1)	Deterministic N-1	Shared structures $>$ 30-50 km	Stressor-based threshold
German TSOs	Extended (n-1)	Curative operations	Netzboosters / Auto-remedial

Table 2.1: Comparison of some European TSO contingency management frameworks.

Chapter 3

VAFFEL Framework Methodology

3.1 Bayesian Framework

The core of the proposed methodology is designed to address the inherent uncertainty associated with the structural response of critical infrastructure to extreme environmental events. Rather than relying on static indices, this study adopts a Bayesian updating framework to synthesize multiple sources of information. This probabilistic approach allows for the transition from a fixed, frequentist failure rate to a dynamic model capable of evolving as new evidence becomes available.

By treating the fragility parameters as random variables the Bayesian engine connects knowledge based on theory or normative values with observed empirical data and therefore uses these two kinds of knowledge to produce a calibrated risk assessment that is not just a theoretical representation but a realistic description of the current state of the asset by bridging the gap between the design assumptions made in the structural design process and the actual operational performance of the asset.

$$\underbrace{P(F|W)}_{\text{Posterior}} = \frac{\overbrace{P(W|F)}^{\text{Likelihood}} \cdot \overbrace{P(F)}^{\text{Prior}}}{\underbrace{P(W)}_{\text{Evidence}}} \tag{3.1}$$

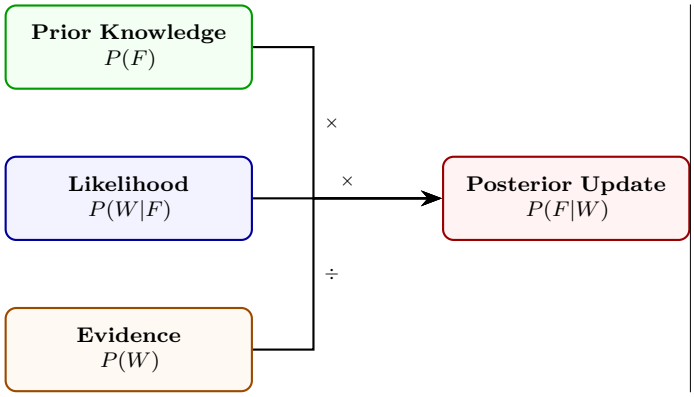

Figure 3.1: Bayesian framework: the mathematical formulation (left) and the corresponding logical data flow (right).

Theoretical Deconstruction of the Bayesian Components:

1. Prior Information about Failure Probability $P(F)$: We use historical data on asset performance over time and what we expect from assets with similar characteristics mechanically, both by type and age at the time of a certain stress event.

2. Probability of Stressors Given Failure $P(W|F)$: This is essentially a structural transfer function that takes the environmental stressors (e.g., wind speed) that are applied to an asset and converts them into failure responses based on the mechanical vulnerabilities of the asset being analyzed.

3. Marginal Evidence $P(W)$: The marginal evidence represents the overall probability of the environmental condition occurring and serves as a scaling factor for the risk update based upon the rarity or frequency of the observed weather event(s).

3.2 The VAFFEL Methodology

The structural integrity of power grid systems can be assessed using the VAFFEL (Vulnerability Assessment for Failure Estimation of Lines) approach [52]. The VAFFEL method represents an operationalization of the Bayesian Engine discussed in the previous section, and therefore provides a structured process for assessing the vulnerability of the electrical distribution network due to environmental influences.

The continuous loop of probabilistic analysis between the static parameters of design of the electrical equipment, and the dynamic conditions of operation, represent the central characteristic of this approach. Additionally, by relating historical performance data with meteorological exposure data, the VAFFEL methodology allows for the calibration of the probability of failure for individual asset types. The subsequent sections will outline the mathematical model for structural fragility and the Bayesian update process.

3.2.1 Update of Failure Frequencies

In the proposed model, the failure rate λ is not assumed as a deterministic constant but is treated as a stochastic variable to account for the inherent epistemic uncertainty. Following the assumption that double-circuit overhead lines fault events are governed by a non-homogeneous Poisson process, the initial uncertainty regarding λ is captured through a conjugate Gamma prior $\Gamma(\lambda)$ [53]:

$$p(\lambda) = \frac{\beta^{\alpha}\lambda^{\alpha-1}e^{-\lambda\beta}}{\Gamma(\alpha)} \tag{3.2}$$

where the shape (α) and rate (β) parameters encapsulate the historical knowledge of the asset class. When empirical evidence becomes available—specifically, a cumulative observation window of n years and a total tally of documented failures ($\sum y_i$)—the model executes a Bayesian update. This refinement yields the posterior parameters:

$$\alpha' = \alpha + \sum y_i, \quad \beta' = \beta + n \tag{3.3}$$

The resulting Bayesian-adjusted failure rate (λ^B), which serves as the statistical pivot for the entire risk assessment, is derived from the expected value of this posterior distribution:

$$\lambda^B = E[\lambda|y, n] = \frac{\alpha + \sum y_i}{\beta + n} \tag{3.4}$$

3.2.2 Construction of The Fragility Curve

The dynamic core of the methodology lies in the non-linear coupling between localized wind velocities (${v_i}^t$) and the system's conditional probability of failure. The mechanical stress exerted on the infrastructure is modeled via a fragility operator, where the effective loading is expressed as a cubic function of velocity, subject to a structural activation threshold (v_{thresh}):

$$\hat{v}_{wind}^{i,t} = \begin{cases} \alpha_w l_i (v_i^t - v_{thresh})^3, & v_i^t \geq v_{thresh} \\ 0, & v_i^t < v_{thresh} \end{cases} \tag{3.5}$$

As established in previous studies, fragility curves quantify the relationship between the weather exposure $\hat{w}$ of a transmission line l and its hourly probability of failure. To translate this physical force into a failure metric, the methodology employs a log-normal Cumulative Distribution Function (CDF). This choice is dictated by the need to represent the variability in material resistance and the uncertainty in load distribution:

$$p_{i,l}^t = F(\hat{v}; \mu_l, \sigma_l) = \int_0^{\hat{v}} \frac{1}{\xi \sigma_l \sqrt{2\pi}} \exp\left[-\frac{\ln^2(\xi/\mu_l)}{2\sigma_l^2} \right] d\xi \tag{3.6}$$

In this formulation, $p_{i,l}^t$ represents the probability of failure for line segment i of line l at time t under the weather intensity $\hat{v}$. The parameters μ_l and σ_l are the location and scale parameters of the underlying log-normal distribution, which effectively map the stochastic intensity of the weather event to the structural response of the infrastructure.

The cumulative vulnerability for a number of N segments of a transmission system as an example of a complex structure is calculated through a weakest link approach to ensure that if a single critical segment fails (either tower or span), the whole transmission system will fail.

Therefore, the equation used to calculate the cumulative probability of a failure over time for each segment of a transmission system is defined by the following:

$$p_l^t = 1 - \prod_{i=1}^{N} \left(1 - p_{i,l}^t\right) \tag{3.7}$$

One important aspect of this process is the calibration of the parameters using the iterative optimization procedure. These parameters (μ_l, σ_l) are calibrated based on the convergence of the temporal mean of the predicted dynamic risk values with the previously adjusted Bayesian historical baseline (λ^B).

This is accomplished using the following equation:

$$\lambda^B \equiv \frac{1}{N_{hours}} \sum_t p_l^t \tag{3.8}$$

This validation checks both that the physical basis of the model is preserved during the adjustment to the specific environment at which the facility is located.

3.3 VAFFEL Limitations

The VAFFEL methodology, as detailed in the preceding sections, provides a robust mathematical foundation for quantifying the structural fragility of overhead lines under stochastic environmental stressors. Through the integration of Bayesian parameter updating and log-normal CDF modeling, the framework effectively reconciles normative design assumptions with empirical failure data. This transition from deterministic constants to calibrated, site-specific failure rates represents a significant improvement in the ability of Transmission System Operators to characterize the vulnerability of individual asset classes.

A major limitation to the methodology employed at present is the static nature of the risk assessment. The "weakest-link" configuration with respect to the mapping of physical forces to structural responses provides a static representation of vulnerability. However, the dependencies that exist within a double-circuit corridor are not captured through this type of analysis. Similarly, the static nature of the assessment does not account for the operational impact associated with repair duration. In particular, the limitations of the fragility approach lie in the inability to model the degraded state-the time period in which a primary circuit failure occurs while the secondary circuit remains in operation. Infrastructure reliability is not solely the absence of failures; it is also the ability to restore service efficiently and to mitigate subsequent cascading events. Therefore, the need exists for a dynamic modeling layer that will transform the static vulnerability assessments to a temporal reliability simulation. To accomplish this, the next chapter introduces a Continuous-Time Markov Chain (CTMC) framework. An extension to CTMC is required to convert static vulnerability assessments to a temporal reliability simulator. Temporal reliability simulators will allow for the explicit evaluation of common cause failures, restoration dynamics and the nonlinear risk accumulation that exists when assessing high-voltage grid operations.

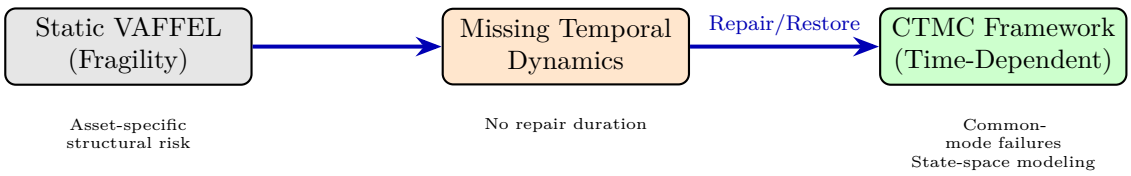

Figure 3.2: Evolutionary path from static VAFFEL fragility to temporal Markovian reliability.

Chapter 4

Markov-VAFFEL Framework Methodology

4.1 Markovian Line Model

To bridge the gap between individual tower fragility and operational service unavailability, I have implemented a Continuous-Time Markov Chain (CTMC) framework. It is critical to note that the “system" under investigation in this research is strictly defined as the double-circuit transmission corridor, rather than the wider regional electrical grid. This approach effectively scales component-level structural risks—such as the failure of a specific tower or span—to the corridor level, allowing for a quantitative assessment of service loss within that specific redundant asset.

The framework models the double-circuit line as a set of interdependent states to explicitly account for redundancy. The model will show how risk evolves over time through its representation of the competitive interaction between the stochastic intensity of failure due to weather and the logistics that restore the system. In doing so, this research differentiates itself from analyses that assess the entire network; by examining the localized processes of one corridor, the model will isolate the effects of common cause failures and localized environmental influences that may be masked when analyzing at a larger scale (the entire grid).

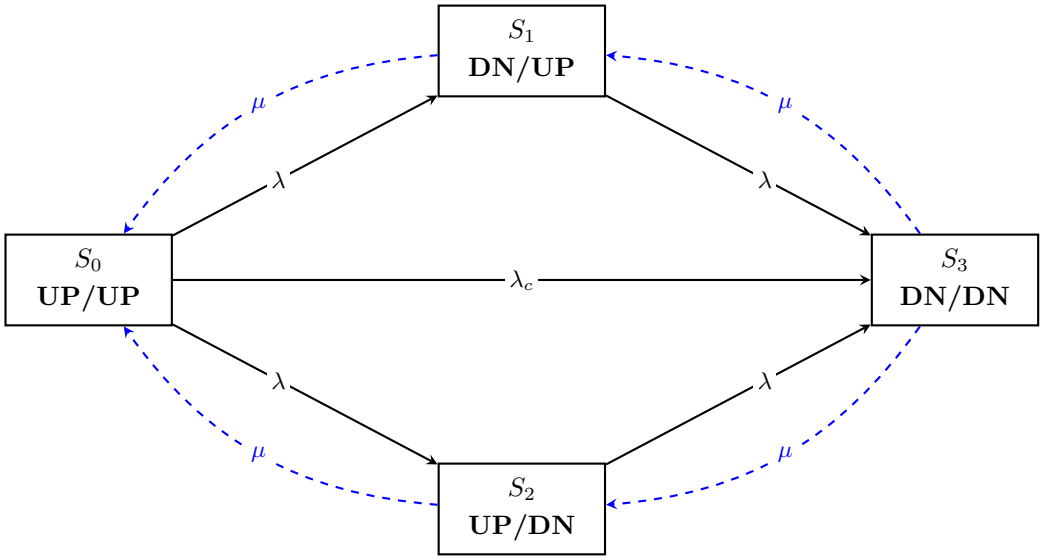

Figure 4.1: State Transition Schematic for double circuit lines.

Solid lines denote failure transitions and dashed blue lines represent restoration paths (μ) in fig. 4.1.

4.1.1 Four-State Framework

For this model, I utilized a 4-state state-space ($\mathcal{S}$) based on the established Nahman-Mijušković framework [54], as seen in fig. 4.1. This representation is necessary to capture the discrete operational phases of a redundant corridor, where the system state $s(t) \in \mathcal{S}$ follows the fundamental reliability logic established for multi-component systems [55]. The number of working circuits determines the state:

1. State 0 (S_0): Both circuits fully operational (full capacity).
2. State 1 (S_1) & State 2 (S_2): One circuit has failed; the system operates with one circuit still functioning (degraded operation).
3. State 3 (S_3): Both circuits have failed (complete outage).

The EHV corridors are physically symmetric. In other words, mathematically, the failure intensities (λ_A, λ_B) and the restoration rates (μ_A, μ_B) for both parallel circuits are equal. This means that:

$$\lambda_A(v) = \lambda_B(v) = \lambda(v); \mu_A = \mu_B = \mu \tag{4.1}$$

The physical symmetry allows us to "lump" the states S_1 and S_2 into one degraded state in some analytical cases (Nahman 1989 [54]) to reduce the complexity of the infinitesimal generator matrix Q while maintaining the logical structure of the double-circuit model. The transition probability from S_0 to the degraded state is therefore 2λ, where λ accounts for the fact that each of the two identical circuits may fail independently. Finally, the symmetry also applies to the Common Cause Failure (CCF) mechanism which plays an important part in the reliability analysis of high-voltage systems [56]. The shared tower body is the common cause failure point that removes the independent redundancy, allowing the system to go from S0 to S3 at a rate $\lambda_c(v)$.

4.1.2 Transition Matrix (Q)

The underlying stochastic engine solves the infinitesimal generator matrix Q, which encapsulates all possible state transitions within the EHV corridor. Each element $q_{i,j}$ represents the instantaneous transition rate from state S_i to state S_j. To ensure the conservation of probability, the matrix is constructed such that the sum of each row is identically zero, with the diagonal elements $q_{i,i}$ representing the total exit rate from state S_i [55].

$$Q = \begin{pmatrix} -(2\lambda + \lambda_c) & \lambda & \lambda & \lambda_c \\ \mu & -(\mu + \lambda) & 0 & \lambda \\ \mu & 0 & -(\mu + \lambda) & \lambda \\ 0 & \mu & \mu & -2\mu \end{pmatrix} \tag{4.2}$$

The failure rates, λ and λ_c are considered to be constant values. However, since failure rates will vary based on the wind speed, the transition matrix Q(v) is recomputed at each point in time with respect to the wind speed profile. This captures the non-linear "risk acceleration" experienced during the development of a storm.

In the first row, we have the fully functional state, S_0. The system may exit S_0 by means of an independent failure of either circuit $(\lambda + \lambda)$ or by means of a simultaneous structural collapse of the common tower body (λ_c). Thus, the overall departure rate of S_0 is -$(2\lambda + \lambda_c)$.

We have the two degraded states, S_1 and S_2 in rows 2 and 3. In either case, there are two possible ways for the system to transition out of these states. Either the system can recover to the fully functional state (at rate μ), or it may experience a failure of the remaining circuit (at rate λ), resulting in complete system failure. As the probability of both independent circuits transitioning states simultaneously is very low in a continuous time Markov chain, q_{12} and q_{21} are set to zero.

We have the total outage state, S_3 in row 4. In this representation, recovery from a total outage is represented by a parallel restoration process ($q_{31} = \mu$ and $q_{32} = \mu$). In this process, the system recovers to its fully functional state via either of the degraded states, which reflects the practical realities of repairing high voltage transmission lines [54].

4.1.3 Steady-State Solutions

The long-term behavior of the transmission corridor is determined by the stationary probability vector $\pi = [\pi_0, \pi_1, \pi_2, \pi_3]$, which represents the asymptotic state occupation probabilities as $t \to \infty$. This vector is derived by solving the system of global balance equations, under the condition that the rate of entry into each state equals the rate of departure:

$$\pi Q = \mathbf{0}, \quad \text{subject to} \quad \sum_{i=0}^{3} \pi_i = 1 \tag{4.3}$$

The system availability metrics are then defined as follows:

- Steady-State Unavailability (p_F): This metric is defined as the probability of the system residing in the total outage state (S_3). Numerically, $p_F = \pi_3$. This value is obtained by solving the linear system $\pi Q = \mathbf{0}$ via numerical decomposition within the engine.
- Mean Time To Failure ($MTTF_{sys}$): This metric measures the expected duration the system remains within the operational subset $\mathcal{S}_{op} = \{S_0, S_1, S_2\}$ before transitioning to the total outage state S_3. By treating S_3 as an absorbing state, we define the sub-generator matrix Q_{trans} by excluding the fourth row and column of Q. The system endurance is then calculated using the fundamental matrix of the absorbing Markov chain [55]:

$$MTTF_{sys} = \mathbf{1}^T(-Q_{trans})^{-1}\alpha \tag{4.4}$$

where $\alpha = [1, 0, 0, 0]^T$ represents the initial state vector (fully operational system) and $\mathbf{1}$ is a column vector of ones.

These metrics provide a comprehensive risk profile: while p_F quantifies the frequency of service loss, the $MTTF_{sys}$ serves as an indicator of temporal resilience. Together, they allow for a rigorous comparison of structural configurations, providing a standardized basis for evaluating corridor endurance under varying meteorological stress intensities..

4.1.4 Conditional Probability of the Degraded State

While steady-state unavailabilities (p_F) provide a long-term behavior overview, they often mask the acute operational risks during storm events. To address this, the framework evaluates the Conditional Probability of Failure, which quantifies the likelihood of a total system outage given that one circuit has already been tripped.

Mathematics of the Degraded State

The ability for the corridor to recover when it has entered a degraded state (either S_1 or S_2), relies on whether the stochastic competition between the logistical restoration rate μ and the weather dependent failure intensity $\lambda(v)$, will be won by the latter prior to recovering to full operation (S_0).

The probability that total outage (S_3) will occur prior to recovery to full operation (S_0), is determined by the transition rates contained within the Generator Matrix Q, as follows:

$$P(F|S_{deg}) = \frac{q_{1,3}}{|-q_{1,1}|} = \frac{\lambda(v)}{\lambda(v)+\mu} \tag{4.5}$$

The ratio described above; denoted as the Conditional Probability of the Degraded State, represents an important diagnostic metric. Because the Steady-State Probability does not account for the Mean Time To Repair ($MTTR = 1/\mu$), the Conditional Probability is significantly more sensitive to the MTTR than the Steady-State Probability. As the wind speed increases and thus causes an increase in the failure intensity $\lambda(v)$, the ratio non-linearly approaches unity and captures the "risk jump" phenomenon where the environmental stress $\lambda(v)$ overwhelms the restorative capacity (μ).

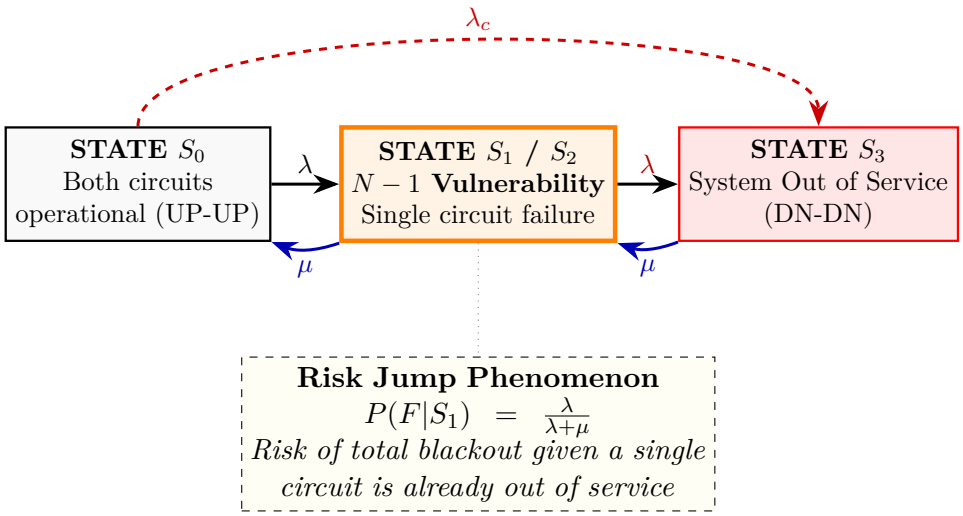

Figure 4.2: State transition block diagram.

4.2 The VAFFEL-Markov Bridge

While the VAFFEL method provides a robust estimation of component-level fragility at discrete wind intensities, it remains essentially a static tool. It quantifies the likelihood of a structural collapse for a given load, but it does not account for the temporal dimension of a storm: it cannot characterize the system's recovery dynamics, the duration of its degraded states, or the way failure risk compounds over the hours of a meteorological event.

To capture the true operational resilience of an EHV corridor, we require a Continuous-Time Markov Chain (CTMC) framework. This transition allows us to move beyond a binary failed or operational paradigm and model the corridor as a dynamic system that evolves continuously.

4.2.1 Coupled Vulnerability (λ_c)

Real-world EHV transmission systems have one major limitation on their ability to share fault-tolerant design concepts due to the use of the same tower for each circuit. The CCF rate $\lambda_c(v)$, introduced via the Markovian integration process, extends the basic independent failure models by modeling the likelihood of an outage of both circuits when the supporting structure that they are mounted upon fails, a possibility that traditional weakest link logic can not represent. The system therefore transitions from a series of independent probability states to a coupled dynamic state where a single wind speed simultaneously causes both independent circuit outages (λ) and structural collapse (λ_c). The relative levels of these failure rates and the repair/ restoration rate (μ) determine how long the system survives and provide a solid base for analyzing system availability.

4.2.2 Relating Structural Fragility to Transition Rates

The most significant obstacle to integrating the VAFFEL structural assessment into a stochastic state-space model is the difference in time scales; the VAFFEL structural assessment provides a discrete probability $P_f(v)$ of component failure as a function of wind load, and this represents a static picture of the risk of failure at a particular wind load. In contrast, the CTMC method requires instantaneous transition rates $\lambda(v)$ that define the movement of the system through its state space.

The VAFFEL output $P_f(v)$ is a cumulative measure, implicitly tied to a specific time interval Δt over which structural stress is evaluated. If we were to use $P_f(v)$ directly as a transition rate, we would violate the Poisson nature of the stochastic process. To bridge these domains, we model the failure process as a time-homogeneous Poisson process within each observation window Δt:

$$P_f(v) = 1 - e^{-\lambda(v)\Delta t} \implies \lambda(v) = -\frac{\ln(1 - P_f(v))}{\Delta t} \tag{4.6}$$

This logarithmic mapping is superior to a naive linear approximation ($\lambda \approx P_f/\Delta t$) for three critical reasons:

- Mathematical Fidelity: The Taylor expansion $\lambda\Delta t = P_f + \frac{P_f^2}{2} + \dots$ demonstrates

that linear models systematically underestimate risk as P_f increases during extreme wind events.

- Asymptotic Consistency: The model is able to approximate the mathematical boundary of the model when collapse occurs; i.e., $\lim_{P_f \to 1^-} \lambda(v) = +\infty$. The singularity in the model indicates the point at which certain failure (collapse) will occur, and no linear model can replicate such a phenomenon.

- Dynamic Sensitivity: By creating this connection, the model transforms the static VAFFEL curves into a dynamic, time-dependent operator $Q(v)$. Thus, it is possible for the system to capture the nonlinear nature of the Risk Jump; that is, the failure intensity increases exponentially with increasing wind speed.

Table 4.1: Mathematical Divergence: Linear vs. Logarithmic λ ($\Delta t = 1h$).

Hazard Level	VAFFEL P_f	Linear λ	Logarithmic λ	Error Ratio
Nominal	≈ 0.00	0.0000	0.0000	1.00
Moderate	0.10	0.1000	0.1054	1.05
Critical	0.50	0.5000	0.6931	1.38
Collapse	0.99	0.9900	4.6052	4.65

4.3 Conclusion

In this chapter, we have created an analytical model that moves from the traditional line-specific static fragility assessment to the corridor-wide dynamic assessments. This is done through the use of a CTMC state space model that captures how the double-circuit line evolves as it goes from being fully loaded (and available), to being degraded (i.e., partially loaded or partially unavailable), to being completely outaged.

We also have used our model to identify steady-state availability as a major source of risk and to isolate the expected time until the system fails by calculating it for each operational state subset using the sub-generator matrix in eq. (4.4). One of the most significant results of our study was the need for a logarithmically mapped method to translate the static fragility curves into instantaneous transition intensities.

The main benefit of using a logarithmic map is to ensure that there is no loss of accuracy due to the linear approximation of the true relationship between environmental stress and transition rate. The linear approximation may systematically underestimate the level of risk at high levels of environmental stress, which can lead to catastrophic failure of the system. Our analytical model will enable us to determine when the occurrence of weather-induced contingency events will be so frequent that they will overwhelm the ability of the power delivery system to recover, which will enable the development of a diagnostic engine for the georeferenced case study of the Sicilian transmission grid to be developed in subsequent chapters.

Chapter 5

Building up study case for contingency analysis

5.1 Study Case Formulation

In the previous chapter we derived the mathematical equations to describe the behavior of the Transmission System; in this one we will discuss the empirical setup needed to test the validity of the VAFFEL-Markov Methodology. We have already seen how to define the Q-matrix (chapter 4) but in order to run a simulation we need a representation of the structure of study assets. We therefore intend to pass from generalised matrices to a geo-referenced structural model of the Sicilian Transmission System. This approach also takes into account the mechanical characteristics of the lattice steel towers of the grid and the topographic limitations of the 220-380 kV corridors. Moreover, we will relate each segment of a line to localised wind conditions, and thus to site-specific climate loads, see eq. (3.5).

Data Integration Layer

As mentioned above, the lack of historical failure data for EHV systems represents a major issue when trying to use the proposed method. In order to tackle this problem, we will present a data integration process. This process involves the combination of three different layers to build up a typical operating environment:

- Grid Topology: Description of the topology of the regional corridors including their spatial and mechanical description. It focuses on the common structural weaknesses of double-circuit towers.
- Wind Exposure: Ingestion of high resolution meteorological data to supply the hourly wind intensity vectors required to determine the failure rates.
- Synthetic Fault Generation: A module to generate an operating history (duration of the synthetic fault generation process is user selectable in the program itself) by linking structural failures with actual meteorological peaks. Alternatively, documents containing the whole historical faults of the studied grid are acceptable.

By describing these steps, this sections will prepare the "input layer". The next chapters will describe the datasets and the heuristics used to calibrate the model, such that the results shown in (chapter 6) refer to the physical and geographic context of the Sicilian area.

5.2 Justification for the Sicilian Study Case

The selection of the Sicilian extra-high voltage (EHV) grid as the primary case study for this research is driven by its strategic importance within the Mediterranean energy transition and its unique exposure to extreme meteorological stressors. As a critical transit hub connecting Mediterranean generation nodes to the Italian mainland, the stability of Sicily's 220 kV and 380 kV grid is essential for maintaining national grid resilience.

5.2.1 Aerodynamic Isolation and Mechanical Stressors

Unlike transmission networks in Northern Europe or the Alpine regions, the Sicilian grid experiences negligible snow or ice accumulation on its 220 kV and 380 kV assets. This climatic characteristic is fundamental to this research, as it allows for the isolation of aerodynamic load as the dominant mechanical stressor. By removing confounding variables such as ice-weight accretion or thermal conductor sag, the Sicilian grid provides an ideal baseline for validating the causal relationship between high-velocity wind events and structural failure.

5.2.2 Topological and Strategic Significance

The topological configuration of the Sicilian grid serves as an ideal environment for modeling redundant corridors. The 220 kV loop effectively encircles the island, facilitating high-capacity power transit between western generation nodes and eastern load centers. This is supported by critical double-circuit infrastructures, such as the 244.85 km Sorgente-Misterbianco corridor, which exemplifies the scale of the island's transmission assets.

Furthermore, the complexity of local wind patterns is uniquely exemplified by the Strait of Messina. Corridors such as the Sorgente-Villafranca-Scilla-Rizziconi interconnector face some of the highest wind-induced failure intensities observed within the national grid. These corridors act as "stress concentration points," making them ideal candidates for testing the VAFFEL-Markov framework under non-linear aerodynamic loading.

5.2.3 Data Fidelity and Meteorological Reanalysis

The validity of this case study is underpinned by the availability of the MERIDA HRES dataset. This high-resolution meteorological reanalysis, specifically optimized for the Italian domain, provides the necessary temporal and spatial granularity to map structural simulations against high-fidelity historical weather patterns. The integration of MERIDA data ensures that the structural simulations presented in subsequent chapters are grounded in a representative environmental context, minimizing epistemic uncertainty in the assessment of failure intensities.

5.3 Topological Extraction and Asset Classification

The reconstruction of the Sicilian 220/380 kV grid is performed through a selective parsing of the dataset. This stage represents a critical data-engineering transition, transforming fragmented geospatial metadata into a unified topological model.

5.3.1 From Raw JSON to Unified Grid

To enable a meaningful resilience analysis, a custom processing pipeline was developed to perform Topological Aggregation. This logic is visualized in fig. 5.1.

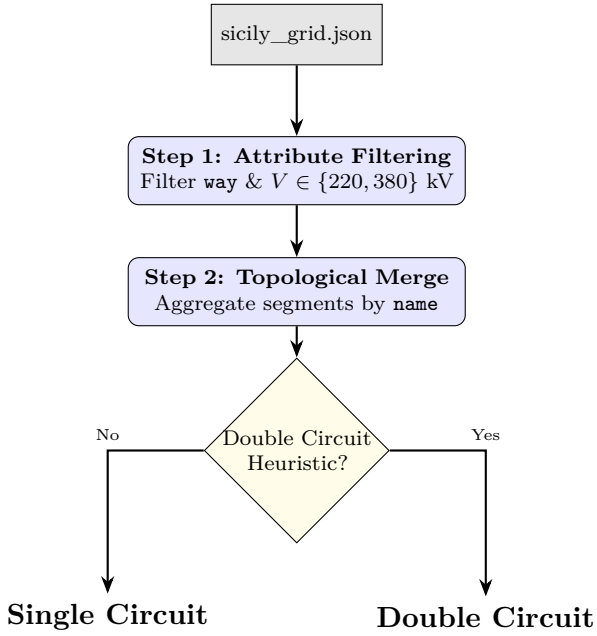

Figure 5.1: Computational workflow for the extraction and classification of Sicilian grid assets.

5.3.2 Geospatial Mapping

In terms of the final output of the topology-extraction process, we have a georeferenced map of the Sicilian 220/380 kV grid; this will serve as the base spatial layer for the integration of the detailed topological structure of the grid with detailed high-resolution meteorological information in order to be able to assess at a fine granularity how vulnerable the overall system is to adverse weather events.

As mentioned earlier, the generation of these heat maps requires a two-stage time-series analysis. In the first stage, the framework computes a long-term climatological average of the wind speeds over the entire nine-year period of the study (2012–2020). Next, the framework computes an annual anomaly by taking the difference between the long-term average of the wind speeds and the average of the wind speeds for each individual year. The use of a differential approach in computing the anomalies eliminates the static effects due to the terrain, thus allowing the identification of those years which experienced extreme meteorological stress.

- Anomaly Distribution: The heat map shows that there are non-uniform wind stress patterns across the island, and identifies some of the corridors that show persistent positive anomalies compared to the historic mean (e.g., the North-Eastern Transit Zone). The results confirm that static failure rates are insufficient for long-term planning since the exposure to meteorological stress due to the topographic complexity of the island varies significantly.

- Exposure of Loop and Grid Elements: The data regarding the wind anomalies indicates that the 220 kV loop that surrounds the island is exposed to different degrees of wind stresses. By mapping the grid elements onto the wind field, the VAFFEL framework is able to identify the grid elements that are subject to the highest stresses and to prioritize repair efforts based on the severity of the exposures rather than simply assessing the risk to the grid as a whole.

- Semantic Differentiation and Asset-Specific Fragility Models: The ability of the VAFFEL framework to semantically differentiate between the 380 kV lines (solid lines) and the 220 kV lines (dashed lines), and to do so at the level of detail provided by the WGS84 grid, enables the framework to utilize asset-specific fragility models for the physically shared infrastructure. As such, the VAFFEL framework can accurately model the joint probability of failure for the physically shared lines under extreme wind conditions.

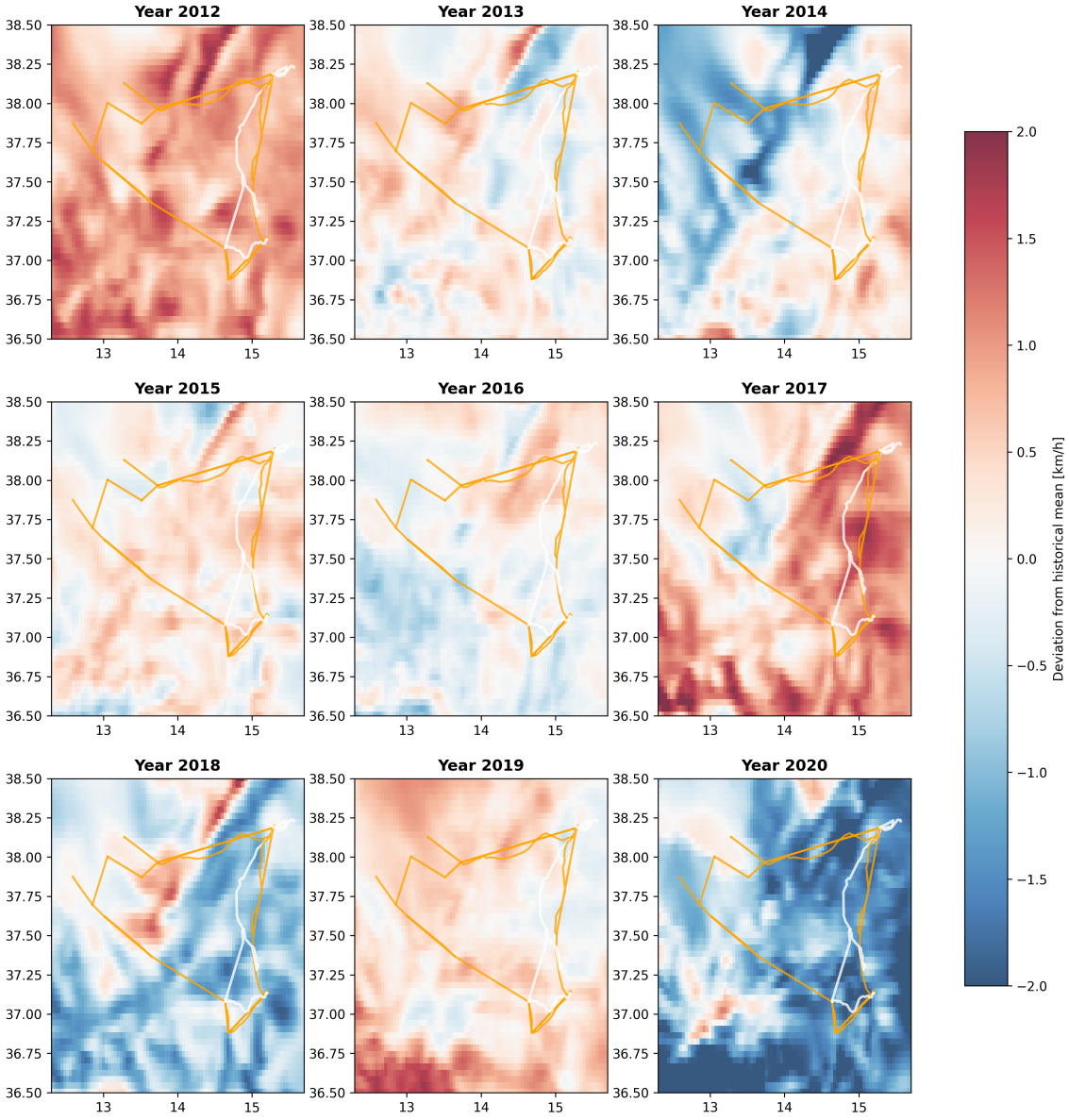

Figure 5.2: Spatial wind speed anomaly distribution across the Sicilian grid from 2012 to 2020.

5.4 Meteorological Data Integration

The quantification of structural risk across the Sicilian grid requires the synchronization of the georeferenced grid model with high-resolution atmospheric data. This study utilizes the MERIDA HRES (MEteorological Reanalysis Italian DAtaset), a product specifically optimized for the Italian domain with a horizontal resolution of 0.04° (≈ 4 km) and a temporal granularity of 1 hour.

Table 5.1: MERIDA HRES Dataset Specifications.

Parameter	Value
Domain	Italy (lon: 5.84–18.96; lat: 35.37–48.25)
Horizontal Resolution	0.04° (≈ 4 km)
Grid Type	Regular Lat-lon
Temporal Resolution	1 hour
Analysis Period	2012 – 2020
Primary Variables	UV100 (U/V Wind at 100m)

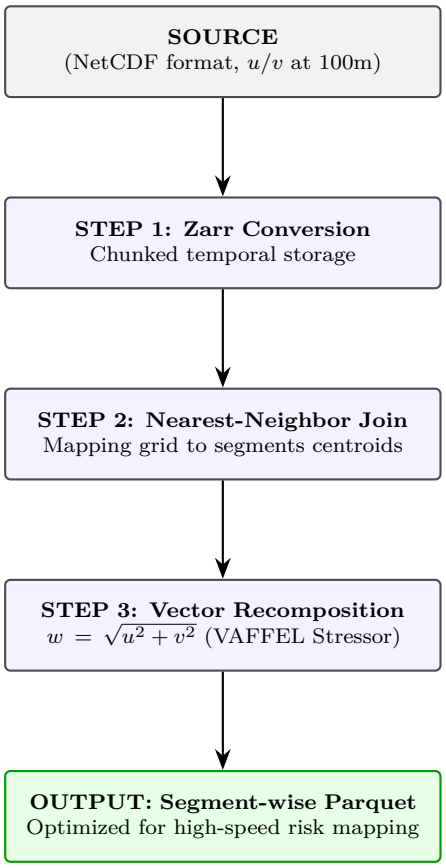

Figure 5.3: The ETL (Extract, Transform, Load) pipeline for merging meteorological data with grid topology.

5.4.1 Source: Dataset Specifications

Table 5.1 summarizes the technical characteristics of the meteorological source used for the risk assessment.

5.4.2 Step 1: The Zarr Transformation

The NetCDF files generated by this analysis (2012-2020) will be an enormous number of files. A conversion pipeline has been set up to convert these raw NetCDF files to Zarr, in order to improve the efficiency of computing. The use of Zarr offers two important benefits; first it can organize data into chunks that are as large as 366×24 hours and therefore greatly speed-up the ability to extract time series data rapidly; secondly, it supports the use of parallelism for Dask operations that can operate concurrently.

5.4.3 Step 2: Nearest-Neighbor Join

The logic implemented, maps the UV100 variables to the transmission grid. Since the MERIDA grid and the electrical corridors do not share identical coordinates, a nearest-neighbor join is performed. This process assigns the wind components of the closest meteorological centroid to each 220 kV and 380 kV line segment.

5.4.4 Step 3: Vector Recomposition

Once the spatial join is complete, the individual u and v wind components are recomposed to determine the magnitude of the wind vector. This step is essential for the VAFFEL method as it defines the primary mechanical stressor acting on the lattice steel towers.

5.4.5 Output: Segment Parquet File

The last part of the ETL process includes placing the processed data in segment-wise Parquet files to allow for rapid reads from large amounts of structured data necessary for the risk mapping and optimization processes. These files will be used directly during the Bayesian update phase to provide a direct connection between the grid topology based on geographic location and the historical wind exposure information. The Parquet file was chosen due to its ability to preserve structural integrity while reading data at high speeds.

5.5 Synthetic Incident Data Generation

The scarcity of historical failure data for high-voltage transmission lines presents a significant barrier to traditional statistical modeling. To overcome this, a module was developed to synthesize a virtual failure history. This engine ensures that the simulated incidents are not merely random occurrences but are grounded in both normative failure benchmarks and local meteorological reality.

5.5.1 Phase 1: Normative Failure Rate Decomposition

The generation process begins by establishing the "budget" of failures for each line over the study period (specifically 2012–2020). I assumed that failure occurrence follows a non-homogeneous Poisson process, which is the standard mathematical model for rare, independent events in engineering systems.

For each transmission line of length L, the total expected number of failures (N_{total}) is split into two distinct categories using the wind incident factor ($\alpha_{inc} = 0.8$):

- Wind-Induced Failures (N_{wind}): Representing 80% of the normative risk, these are failures directly tied to atmospheric stress. This value selection is justified by established benchmarks for Extra-High Voltage (EHV) overhead lines. According to [57], meteorologically induced events account for 70% to 90% of all transmission line outages in mature networks. In the specific context of the Sicilian grid, where the incidence of snow or ice accumulation on the 220 kV and 380 kV grid is negligible, the primary structural stressor is aerodynamic load. This 80/20 split is further supported by European TSO data (e.g., Statnett [58]) and reliability studies in Mediterranean climates, where wind gusts are the dominant cause of structural failure [59].
- Residual Failures (N_{other}): Representing 20% of the risk, these account for incidents unrelated to wind, such as technical degradation, lightning, or vegetation interference.

The expected values are calculated as:

$$E[N_{wind}] = L \times (\lambda_{norm} \cdot \alpha_{inc}) \times n, \quad E[N_{other}] = L \times (\lambda_{norm} \cdot (1 - \alpha_{inc})) \times n \tag{5.1}$$

5.5.2 Phase 2: Meteorological Coupling

The core innovation of this script is its “Temporal Coupling” logic. While N_{other} incidents are distributed uniformly at random across the 9-year timeline, N_{wind} incidents are physically anchored to the wind data.

For every line, the script identifies the top 1% of wind speed hours recorded in the pre-calculated Parquet dataset. When a wind-induced failure is generated, the script samples a timestamp specifically from these peak hours. This prevents a "wind failure" from being assigned to a calm day. By forcing failures to coincide with the most intense 1% of weather events, the synthetic dataset respects the physical law that structural collapse occurs at the limits of structural demand.

5.5.3 Phase 3: Failure Modes

The grid uses mostly double-circuit lines with one shared tower; therefore, the simulation has to consider Failure Bunching. The Common Mode Probability ($P_{cm} = 0.20$), in this case, is used by a script to assess the effects of a trip:

- 80% Independent Failure: Random selection of either circuit (1 or 2). This represents a localized component failure like an insulator flashover that would not have affected the other circuit.
- 20% Common Mode Failure: Both circuits are tripped at the same time.

5.5.4 Implemented Workflow

The following flowchart illustrates the sequence of operations, from the ingestion of global parameters to the final generation of the Excel-formatted incident log.

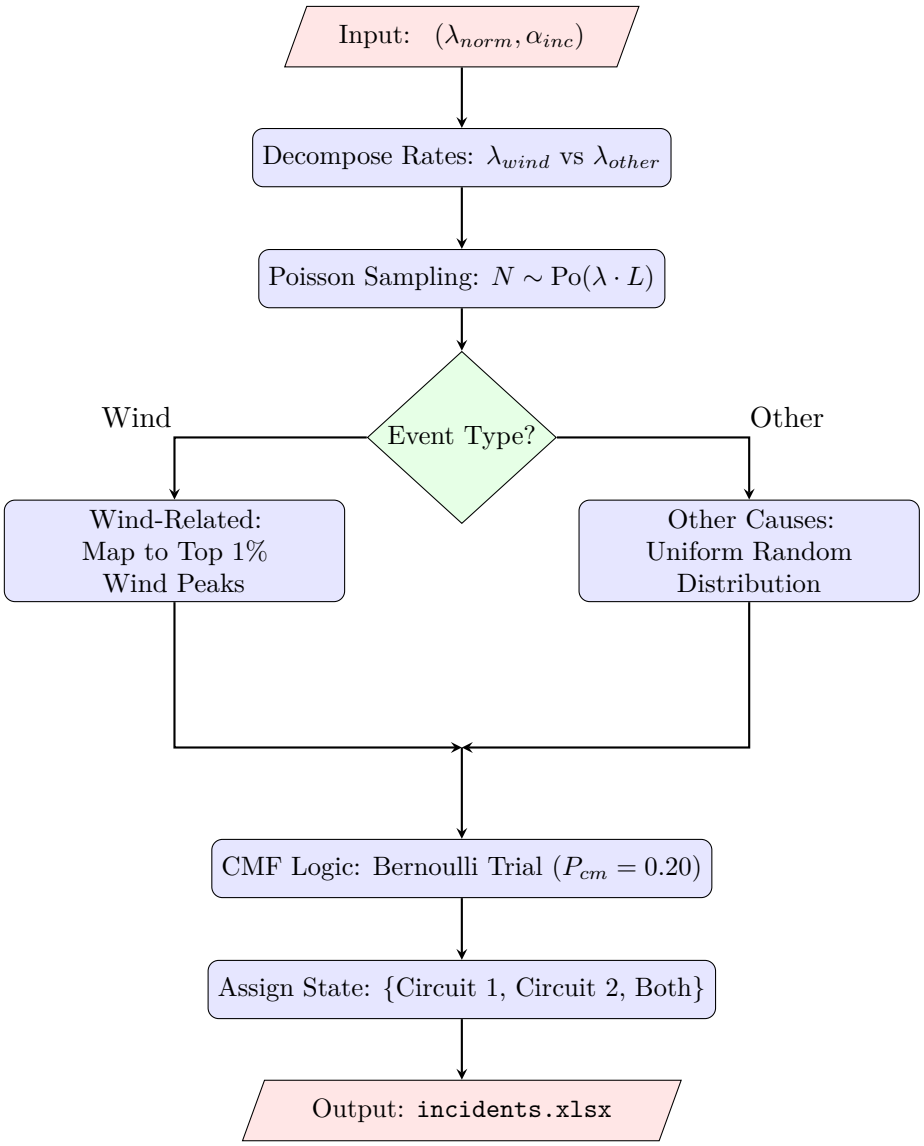

Figure 5.4: Syntethic Incident Generation workflow focusing on Sicilian double-circuit assets.

Chapter 6

Analysis of EHV double circuit: Sicilian Case

6.1 Introduction

This chapter executes the analytical framework established in chapter 4, transforming the theoretical VAFFEL-Markov framework into a quantitative assessment. By applying the synthetic failure history created in section 5.5, I evaluated the performance of each line under wind-induced loading.

The structural and operational baseline for the analyzed assets is summarized in table 6.1 , where the nominal design limits are contrasted with historical peak events.

Table 6.1: Sicilian Double-Circuit Line Profiles and Design Thresholds (2012–2020).

ID	Line Name	kV	Len. [km]	Faults	V_{ULS} [km/h]
1	Chiaramonte Gulfi-Ragusa/1-2	220	22.76	0	140.0
2	Corriolo-Caracoli/Sorgente	220	145.33	9	140.0
3	Corriolo/Caracoli-Sorgente (s)	220	0.90	0	140.0
4	Melilli-Ragusa/1-2	220	52.31	5	140.0
5	Misterbianco-Melilli/1-2	220	48.10	3	140.0
6	Sorgente-Misterbianco	220	244.85	23	140.0
7	Sorgente-Villafranca-Scilla-Rizz.	380	52.40	1	160.0

V_{SLU} represents the Ultimate Limit State wind speed threshold, defined as the structural design load limit for the towers according to CEI EN 50341-1 [60]. This value serves as the boundary condition for the subsequent construction of the fragility curve in my model, for further detail see appendix 1.

6.2 VAFFEL Algorithm Application

In accordance with the Bayesian framework, the model extracts λ_{prior}. A defining characteristic of this implementation, strictly enforced within the computational engine, is the derivation of a specific failure rate associated with wind events:

$$\lambda_{wind} = \lambda_{prior} \cdot \alpha_{inc} \tag{6.1}$$

By setting $\alpha_{inc} = 0.8$ (see section 5.5.1), the framework assumes that 80% of the national normative failure rate is attributable to wind-driven structural stress.

This isolation is a prerequisite for the VAFFEL method, ensuring the Bayesian update is not diluted by non-climatic faults—such as maintenance errors—which do not contribute to the mechanical degradation of the tower structure [52].

6.2.1 Bayesian Framework

The transition from theoretical modeling to the Sicilian Case Study begins with the initialization of the Bayesian Framework. As established in section 3.1, the model does not treat failure rates as static constants but as dynamic variables updated by historical and environmental evidence. This section details how the computational engine processes the prior tower information and the wind data to calibrate the safety of the 220 kV and 380 kV corridors.
Bayesian hyper-parameters are set according to [53]. Failure rates are derived from high-voltage equipment performance benchmarks [61].

6.2.2 Asset Failure Frequency

Table 6.2: Setting Parameters for the Bayesian Framework.

Parameter	**Value**	**Unit**
λ_{prior} (220 kV)	0.00730	[failures/(year $\cdot$ km)]
λ_{prior} (380 kV)	0.00340	[failures/(year $\cdot$ km)]
α_{prior}	1.0	[−]
β_{prior}	$\frac{1}{\lambda_{prior}}$	[−]

The real strength of the VAFFEL framework lies in how it handles the failure rate λ [failures/year]. Instead of applying a flat rate across the board, the model scales the expected failure rate based on the actual size of each asset, using the line length L as a direct multiplier:

$$\lambda_{asset} = \lambda_{prior} \cdot L \tag{6.2}$$

This approach is essential because a massive corridor, such as the Sorgente-Misterbianco line (244.85 km), is physically more exposed to local weather extremes than a short segment like the Chiaramonte Gulfi-Ragusa line (22.76 km). By incorporating line length directly into the calculation, the model immediately captures the scale of the infrastructure. This ensures that the Bayesian update process starts from a realistic, asset-specific baseline, making the entire model significantly more accurate across the high-voltage grid.

6.2.3 Prior Failure Rates vs. Updated

The results reported in table 6.3 result from the combination of the Bayesian updating process of the failure rate and the analytical relationship between the normative priors and empirical evidence. The posterior failure rate is determined using a Gamma-Poisson conjugate framework. It is established by the ratio of recorded fault frequencies to total exposure time (observation window), and therefore it represents a weighted average of the two parameters. In case of corridors with many faults, i.e., Sorgente-Misterbianco, the large number of faults observed during the analysis influences the calculation of the posterior rate with an increase of 44.2%. The recorded fault frequency is higher than the one used as a prior; therefore, it is necessary to use a more conservative risk assessment. On the other hand, when there are no faults recorded, i.e., Chiaramonte Gulfi-Ragusa, the posterior rate is lower (-54.5%) because the longer the observation period is, the more diluted the prior will be, and the greater the reward for having operated without fault. The model also considers the mechanical stress of the structures due to their design features, through the application of the design limits defined by the Normative Standards. In fact, for the 380 kV Sorgente-Rizziconi line, the posterior rate is lower (-12.4%), as it reflects the higher mechanical design thresholds for towers and lines indicated by the Normative Standards. Finally, the model has also the ability to maintain a certain degree of statistical stability for the 0.90 km long Corriolo/Caracoli segment. The very low value of the posterior rate (-4.5%) shows that the model has identified a lack of exposure, since the product of the length of the considered segment and the observation time is too low to allow any difference from the expected rate. Therefore, the model guarantees the correctness of the fragility assessment and prevents the update of the expected rate from being excessively influenced by limited data samples.

Table 6.3: Bayesian Update Results for Sicilian Double-Circuit Lines (Analysis Period: 2012–2020).

Corridor	**kV**	**Len. [km]**	λ_{prior} **[f/y]**	λ_{post} **[f/y]**	Δ **[%]**
Chiaramonte Gulfi-Ragusa/1-2	220.0	22.76	0.1330	0.0605	-54.5
Corriolo - Caracoli/Sorgente	220.0	145.33	0.8488	0.9825	+15.8
Corriolo/Caracoli - Sorgente (s)	220.0	0.90	0.0052	0.0050	-4.5
Melilli-Ragusa/1-2	220.0	52.31	0.3055	0.3259	+6.7
Misterbianco-Melilli/1-2	220.0	48.10	0.2809	0.2389	-15.0
Sorgente-Misterbianco	220.0	244.85	1.4299	2.0620	+44.2
Sorgente-Villaf.-Scilla-Rizz.	380.0	52.40	0.1425	0.1249	-12.4

6.2.4 Fragility Curve Optimization Process

The optimization engine represents the computational core of the fragility model. It is responsible for linking the Bayesian updated failure rate with the geometric attributes of the log-normal distribution. In contrast to heuristics curve fitting, the optimization engine represents the process of minimizing the difference between the model predicted performance and the statistically inferred failure rate.

Evidence Based Initialization

Given the computational efficiencies of the L-BFGS-B solver and the need for physically relevant results, an evidence based initialization method has been adopted instead of random parameter initialization:

- Empirical Median (μ_{start}): This value is calculated as $\ln(median(V_{faults}))$ for lines that have experienced historical failures. For lines that do not have documented failures, a conservative estimate of $\min(V_{max\_hist} \times 1.05, V_{SLU} \times 0.9)$ is used to represent design specifications.
- Structural Uncertainty (σ_{start}): This value is fixed at 0.22, representing the standard deviation of resistance for steel lattice transmission towers.

Boundary Constraints: The Regulatory Fencing

The optimization is constrained by strict physical bounds to ensure that the solution remains physically realistic:

- Horizontal ($\mu \in [-\infty, \ln(V_{SLU})]$): The horizontal constraint on the median failure wind speed will never exceed the ultimate limit state (ULS) wind speed defined by EN 50341, thereby preventing a potential regulatory disaster.
- Vertical ($\sigma \in [0.15, 0.40]$): The vertical constraints prevent unrealistically extreme step function failures by forcing the lower bound to be greater than or equal to 0.15. Similarly, the upper bound prevents an excessively flat model by requiring the standard deviation to be less than or equal to 0.40.

Optimization Workflow Synthesis

The optimization cycle consists of three distinct components:

1. Targeting: The model targets the posterior failure rate λ_{post}.
2. Iterative Search: The L-BFGS-B solver iteratively searches through the (μ, σ) space, subject to the specified boundary constraints.
3. Convergence: An optimal configuration $(\mu_{opt}, \sigma_{opt})$ is found that meets both the posterior failure rate and is anchored to empirical data by virtue of soft penalty terms (0.1 for μ and 0.05 for σ).

6.2.4.1 No Fault Case Scenario

The explained workflow shows that this deterministic approach anchors every fragility curve to either empirical fault data or normative capacity limits so that as shown by the results, the curves show how this method can distinguish between resilient (high-resilience) assets and structurally vulnerable ones. Anchoring the fragility model to physical boundaries like these allows for numerical stability across all corridors independent of whether the line has an extensive history of incidents or has run throughout the duration of the observation period without incident.

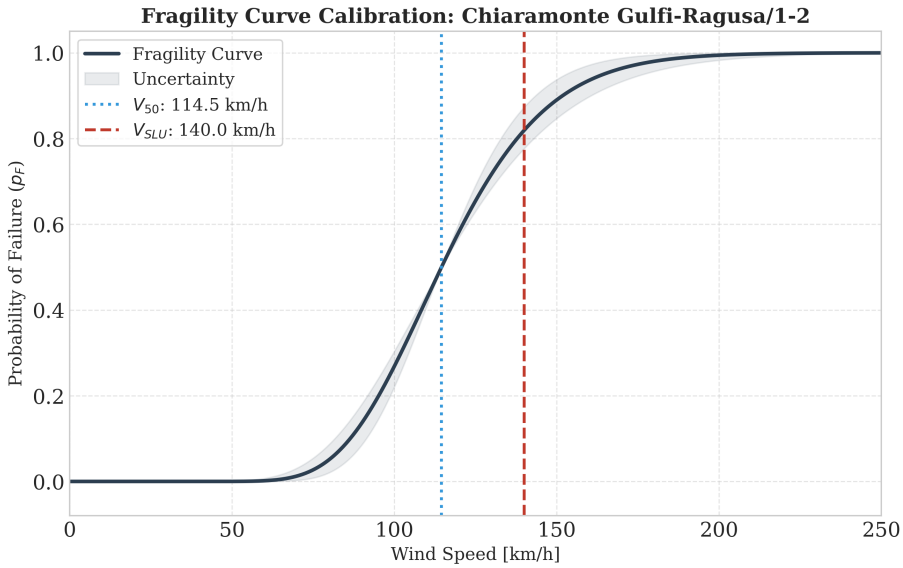

Figure 6.1: Fragility curve of Chiaramonte Gulfi-Ragusa 1-2.

The fragility curve, as seen in fig. 6.1, shows how the total probability of failure (P_f) relates to instantaneous wind speed. A fragility curve is defined by its median collapse velocity ($V_{50} = 114.5$ km/h) where the probability of collapse equals to 50 % and its associated σ (steepness). The shaded area around the curve reflects the uncertainty of the model that has been created due to variability in materials of construction and errors from historical data. Therefore, this shaded area represents a band of confidence of the true failure point of the structure. As indicated by (σ) shows there is little variation in the failure probability when the wind speed exceeds 100 km/h. The failure probability is nearly 90% at the tower design wind speed ($V_{SLU} = 140.0$ km/h). As such, the model shows that the structural integrity of the transmission line is consistent with normative standards, and provides an adequate margin of safety against extreme winds.

6.2.4.2 Fault Case Scenario

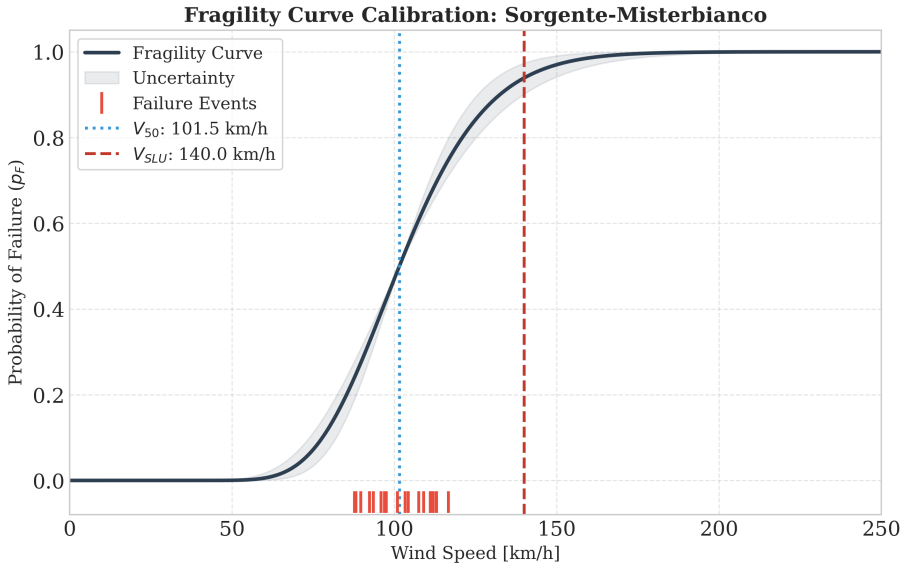

Figure 6.2: Fragility curve of Sorgente-Misterbianco.

The fragility curve for Sorgente-Misterbianco reveals a significant structural degradation. With a Bayesian shift of +44.2%, the model identifies a high concentration of failure events across a wide wind spectrum (87.7–116.6 km/h). The low V_{50} (101.5 km/h) indicates that the asset is operating in a state of chronic vulnerability, where normative design limits no longer reliably mitigate failure risk.

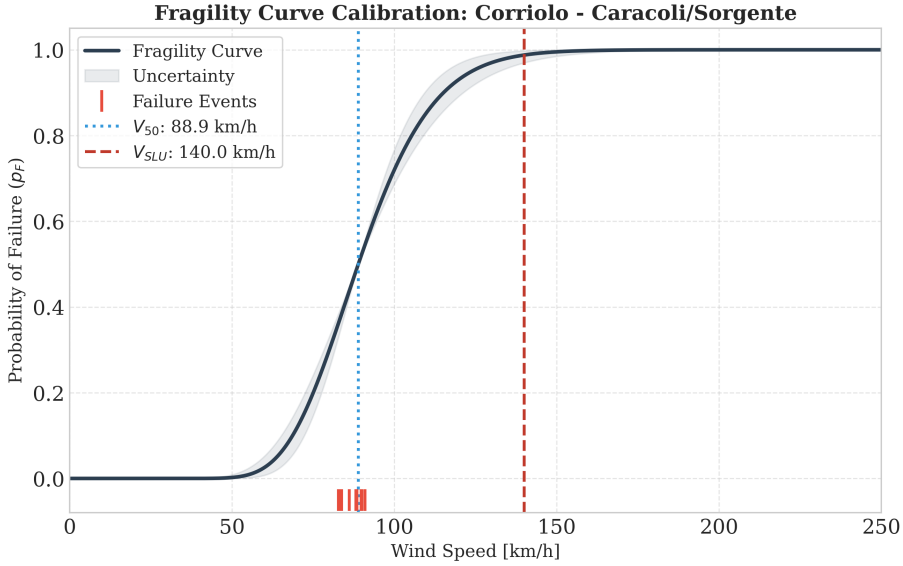

Figure 6.3: Fragility curve of Corriolo-Caracoli/Sorgente.

This asset shows clustered failure events within a narrow, low-velocity band (82.8–91.0 km/h). The moderate Bayesian shift of +15.8% suggests a localized structural sensitivity rather than systemic degradation, pointing to specific mechanical fatigue or terrain-induced wind amplification at lower thresholds.

6.3 Determination of the transient intensity rate

The connection between the VAFFEL fragility model and the Markov process represents the computational heart of this study. This "bridge" maps the discrete probability of failure, $P_f(v)$, obtained from the structural fragility models into a continuous transition intensity rate, $\lambda(v)$, that can be used to construct the infinitesimal generator matrix Q.

Within this framework, the fragility curve acts as the functional relationship between environmental stressors and likelihood of failure. The Bayesian-updated V_{50} serves as the scaling parameter for the fragility curve. A larger V_{50} shifts the curve to the right, thus decreasing the failure probability for a given wind velocity. Therefore, since $\lambda(v)$ is mathematically derived from these probabilities, the V_{50} determines the exact wind speed threshold above which the transition rates in the Q matrix increase.

This guarantees that the structural "memory" of the asset will control the dynamics of the Markov process within the simulated state-space over the course of the simulation.

6.3.1 Coupling of Vulnerability via Common Cause Failures (CCFs)

A Common Cause Failure (CCF), according to IEEE [56], refers to a failure of two or more otherwise independent components due to a single external cause or shared internal dependency.

Therefore, the transition from the VAFFEL fragility model to the Markov-based analysis necessitates the strict quantification of the CCF failure rate, λ_c.

6.3.2 Constant Beta-Factor Model

I employed the Constant Beta-Factor Model [62] to provide evidence for the determination of λ_c. This model breaks down the total failure rate of an asset (λ_{total}) into two separate failure rate components, namely the failure rate of an individual component (λ_i) and the failure rate due to the shared dependence of the two components (λ_c).

Therefore, we have the following two equations:

$$\lambda_{total} = \lambda_i + \lambda_c \tag{6.3}$$

$$\lambda_c = \beta \cdot \lambda_{total} \tag{6.4}$$

where β denotes the proportion of all failures that occur in such a manner that they affect both circuits simultaneously. In the case of high-voltage transmission, this includes the structural failure of the lattice tower or shielding failure of both circuits during a single extreme weather event.
I therefore applied a common-mode probability factor, denoted as $\beta = 0.20$, to account for the effect of the risk due to shared infrastructure. This value is based on an engineering judgment representing a conservative assessment of failure classification methods for EHV overhead lines. The structural collapse, caused by extreme wind gusts or failure of the foundation, is regarded as a non-localized common cause and is classified under the category of local failures. In the absence of proprietary fault-tree data for specific corridors, the

β-factor range of 0.1 to 0.3 has been widely accepted in literature related to power system reliability as indicative of the structural vulnerability of towers subject to global aerodynamic loadings [63].

6.3.3 Failure Rate Function $\lambda(v)$

The stochastic bridge is numerically executed through the conversion of the hourly wind speed data into the continuous transition intensity function $\lambda(v)$. This ensures that the wind data recorded in the MERIDA dataset is properly translated into the Markovian state-space. Although the historical data contains discrete wind speeds, the Markov engine needs a failure rate. As indicated by equation 4.6 for the low probability of failure found in normal weather conditions, $\lambda \approx P_f$. However, as wind speeds are greater than the design limits of the 220 kV and 380 kV towers, the logarithmic transformation ensures the transition intensity accurately captures the nonlinear escalation of structural risk.

6.4 Markovian Model Application

This section describes the numerical application of the Continuous-Time Markov Chain (CTMC) to the Sicilian EHV corridors according to the theory developed in Chapter 4. The CTMC is used to quantify the available number of 220 kV and 380 kV lines under historic conditions of wind-induced stress.

6.4.1 Operationalization of the Four-State Framework

The four-state space $\mathcal{S}$, which has been described in section 4.1.1 (see fig. 4.1) is implemented using the simulation tool for each of the corridors. The four discrete states represent the different possible operating modes of the system:

1. State 0 (S_0): Both circuits are fully operational.
2. States 1 and 2 (S_1, S_2): Degraded operation: The remaining operational circuit will be used to ensure continued operation of the system until one of the two circuits can be restored at rate μ.
3. State 3 (S_3): Full loss of service; the system fails due to either sequential failure of both circuits ($S_1 \to S_2 \to S_3$), or due to a common cause failure of all circuits ($S_0 \to S_3$).

The physical symmetry hypothesis ($\lambda_A = \lambda_B = \lambda$) was maintained in the implementation. The numerical solution of the weather profile's transition probability matrix $P(t)$ at each time step is obtained by solving the infinitesimal generator matrix Q. According to eq. (4.2), Q is composed of the following elements:

$$Q = \begin{pmatrix} -\left(2\lambda + \frac{\lambda_c}{8760}\right) & \lambda & \lambda & \frac{\lambda_c}{8760} \\ \mu & -(\mu+\lambda) & 0 & \lambda \\ \mu & 0 & -(\mu+\lambda) & \lambda \\ \mu_c & 0 & 0 & -2\mu \end{pmatrix}. \tag{6.5}$$

While the restoration rate μ and the common-cause rate λ_c are constant values, the failure intensity $\lambda(v)$ is recalculated every hour. This is to capture the nonlinear increase of risk that occurs when the peak Scirocco event occurs. The diagonal elements q_{ii} of the infinitesimal generator matrix Q describe the rapid growth of exit rates from the operational states.

6.4.2 Line Safety Ranking and Decision Triggers

In this section, the steady-state unavailability results (p_F) are mapped to the operational procedures defined by the Terna Grid Code [64] and EU Regulation 2017/1485 [65]. This classification utilizes p_F as a decision-making trigger to transition between system states, shifting specific contingencies from "out-of-range" to "exceptional" based on increased probability due to environmental factors [64].

Table 6.4: Line Status Classification, Probability Thresholds, and Regulatory Actions.

Status	Symbol	Range (p_F)	Operational Action Level
Normal	⋆	$p_F \leq 10^{-2}$	SCADA/EMS monitoring; Contingency Analysis every 15 min
Alert	■	$10^{-2} < p_F < 10^{-1}$	Preventive Redispatching; Topology optimization; UPDM arming
Emergency	▲	$p_F \geq 10^{-1}$	System Defense Plan (PdD); RIGEDI/PESSE activation

Nomenclature of Primary Protocols: The following nomenclature identifies the specific TSO procedures and technical infrastructure activated by the p_F thresholds, ordered by increasing system risk:

SCADA / EMS: The standard operational state relies on Supervisory Control and Data Acquisition (SCADA) and Energy Management System (EMS) for real-time telemetry and grid monitoring [64, 65]. These systems facilitate continuous state estimation and the execution of contingency analysis at 15-minute intervals to verify that the system remains within security limits [65, 64].

Redispatching / UPDM: Preventive alert measures are triggered by identified contingencies that risk violating operational security limits [65, 64]. Redispatching involves market-based modifications of generation schedules to mitigate congestion [65, 64]. The Peripheral Disconnection and Monitoring Unit (UPDM) allows for the instant extraordinary downward modulation of power plants to prevent system degradation [64].

PdD / RIGEDI / PESSE: Emergency curative protocols are activated when security limits are violated or system integrity is at risk [65, 64]. The System Defense Plan (PdD) integrates specialized measures such as the Procedure for the Reduction of Distributed Generation (RIGEDI) to preserve frequency stability [64]. It also includes the Emergency Plan for System Security (PESSE) for manual load shedding of distribution feeders to prevent total system blackout [64].

Unified Operational Action Matrix

The system's resilience is evaluated across three restoration scenarios (MTTR = 8h, 16h, 32h). As the restoration time increases, the grid shifts from preventive control toward systemic emergency protocols. The TSO operational actions are consistent across all scenarios, triggered by the calculated unavailability (p_F).

Table 6.5: Unified Operational Action Matrix across all MTTR scenarios.

TSO Operational Action	**Normal**	**Alert**	**Emergency**
SCADA/EMS Real-time Monitoring	✓	✓	✓
$N-1$ Contingency Analysis	✓	✓	✓
Preventive Redispatching (Market)	-	✓	✓
UPDM / Defense System Verification	-	✓	✓
Automatic Load Shedding (EAC)	-	-	✓
RIGEDI Procedure Activation	-	-	✓
Manual Load Shedding (BME/PESSE)	-	-	✓

Sensitivity Analysis of Line Corridors

Table 6.6: Unavailability (p_F) and Operational Status per MTTR scenario.

		4h		**8h**		**16h**		**32h**	
Line Corridor	**kV**	p_F	**S.**	p_F	**S.**	p_F	**S.**	p_F	**S.**
Misterbianco–Melilli/1-2	220.0	0.3490	▲	0.5520	▲	0.7270	▲	0.8470	▲
Melilli–Ragusa/1-2	220.0	0.2750	▲	0.4740	▲	0.6650	▲	0.8070	▲
Sorgente–Rizziconi	380.0	0.0295	■	0.0859	■	0.2060	▲	0.3890	▲
Corriolo–Caracoli–Sorgente	220.0	0.0287	■	0.0840	■	0.2020	▲	0.3840	▲
Sorgente–Misterbianco	220.0	0.0025	⋆	0.0088	⋆	0.0293	■	0.0851	■
Chiaramonte Gulfi-Ragusa/1-2	220.0	0.0003	⋆	0.0010	⋆	0.0037	⋆	0.0130	■
Corriolo/Caracoli - Sorgente	220.0	0.0001	⋆	0.0005	⋆	0.0019	⋆	0.0069	⋆

As demonstrated, increasing the MTTR from 8h to 32h forces nearly all corridors into the Emergency State (▲, $p_F > 0.1$). This indicates a preventive manouvres saturation, where local preventive measures (e.g., redispatching, UPDM) are insufficient and large-scale defense plans (PdD) become mandatory to maintain system integrity.

6.4.3 Conditional Probability and Incremental Risk

The incremental risk assessment shown in fig. 6.4 illustrates how the probability of total system collapse evolves for the Sorgente–Misterbianco 220 kV corridor as maintenance windows (MTTR) extend.

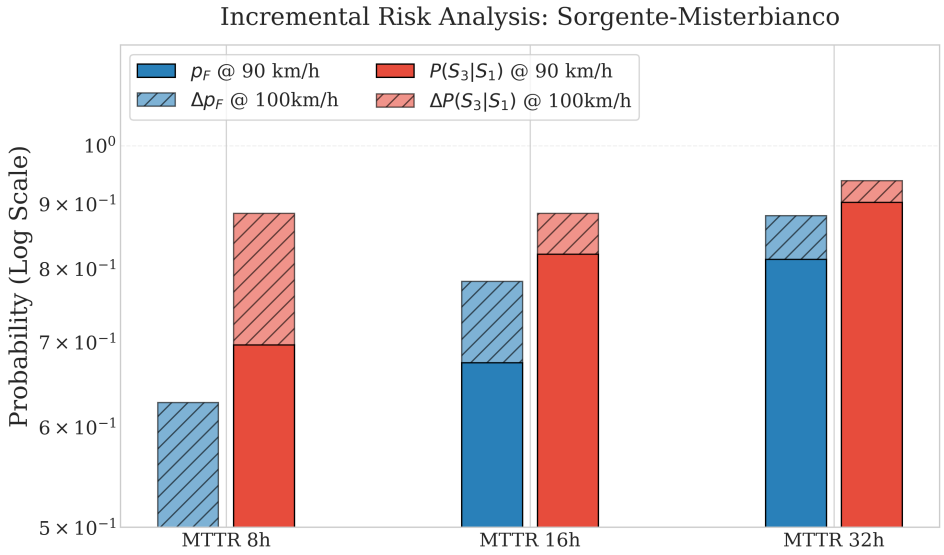

Figure 6.4: Evolution of operational failure (p_F) versus conditional system collapse $P(S_3|S_1)$ at varying MTTR intervals for Sorgente–Misterbianco.

To properly understand the conclusions from the study you need to make a distinction between the two types of probabilities used in this research:

- Structural Vulnerability ($P_f(v)$) = This refers to the fragility curve. The structural vulnerability is the physical chance that the tower will fail as a function of wind speed (v). Therefore, structural vulnerability is a built-in metric of the asset's mechanical durability.
- Failure in Operations (p_F): This is a larger scale representation of what we would consider "real world" risk. In this case, failure in operations includes both the inability of the line to be available, and also the longer term logistical issues associated with the time dependent restoration of the line, i.e. the Mean Time to Repair (MTTR).

These changes illustrate how there is a direct relationship between increased time to repair and decreased operational safety margins.

The risk of the system being saturated with failures, which we refer to as "Risk Saturation" is demonstrated by the increasing trend of Mean Time to Repair (MTTR) from 8 hours to 32 hours, and the constant increase in failure probability. The incremental component Δ shows a relatively smaller change than the baseline component. Therefore, the system reaches a near-collapse scenario, or a limiting risk condition, when it experiences a delay in logistics of up to 32 hours; the difference between a 100 km/h and a 90 km/h wind solicitation becomes statistically insignificant.

Additionally, the degradation of the resilience is shown as the vertical distance between the top of the blue bar, which represents the p_F, and the bottom of the red bar, which represents the conditional probability $P(S_3|S_1)$, decreases as the MTTR increases. This illustrates the degradation of the recovery capability of the system; whereas at 8 hours the event can be considered a manageable single contingency, at 32 hours the uncertainties in the logistical process dominate the system dynamics, making the progression to a full system collapse S_3 nearly deterministically certain. Overall, the analysis demonstrates that for the Sorgente-Misterbianco corridor, there is a fundamental regime shift in the system's stochastic behavior, and the system will reach asymptotically critical failure probabilities, when the time to repair exceeds the 16 hour threshold.

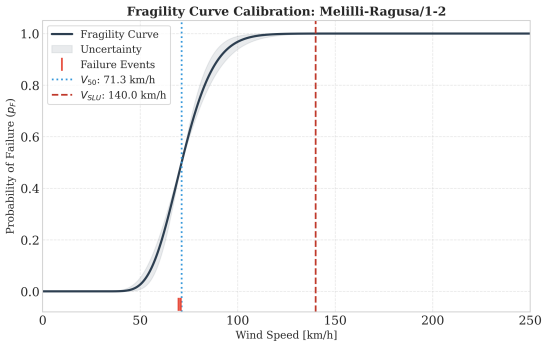

Figure 6.5: Structural Fragility Curve for Melilli-Ragusa 1-2.

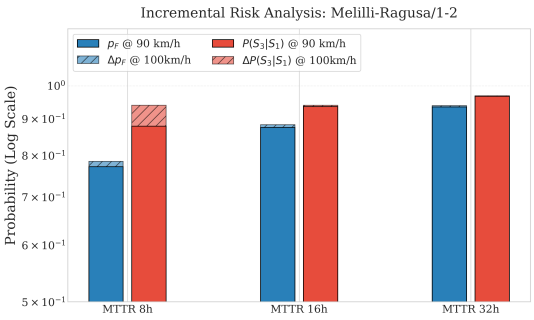

Figure 6.6: Full Incremental Risk Analysis for Melilli-Ragusa 1-2.

The data from the graph in fig. 6.6 illustrate that the close relationship between the structural state of the Melilli-Ragusa 1-2 corridor shown in fig. 6.5 limits the entire performance of the system.

Clearly, the corridor has saturated with regards to fragility since its operational limit (between 90 and 100 km/h) far exceeds the median wind velocity (V_{50}= 71.3 km/h). Therefore, the system operates in the upper portion of the fragility curve and there is a consistent high level of structural failure probability (P_f). This structural vulnerability creates an elevated base level of risk for the system which makes it very susceptible to any initial contingency or loss of any single element in the system.

Additionally, the structural fragility is almost deterministic and as such there is a logistical decoupling of the system. Since the system is so vulnerable, the Mean Time To Repair (MTTR) will be inadequate to mitigate the cumulative risk of the system. As the MTTR increases, the system will spend a larger percentage of its time in a degraded state. Considering that the environmental stress at 100 km/h is already extreme, the likelihood of another event occurring prior to the original fault being repaired is approaching unity.

Therefore, similar to the Melilli-Ragusa 1-2 corridor, the structural redundancy of the system is overpowered by the environmental stress and thus the total system outage (S_3) is virtually certain under these conditions.

6.4.4 Sensitivity of The Conditional Risk

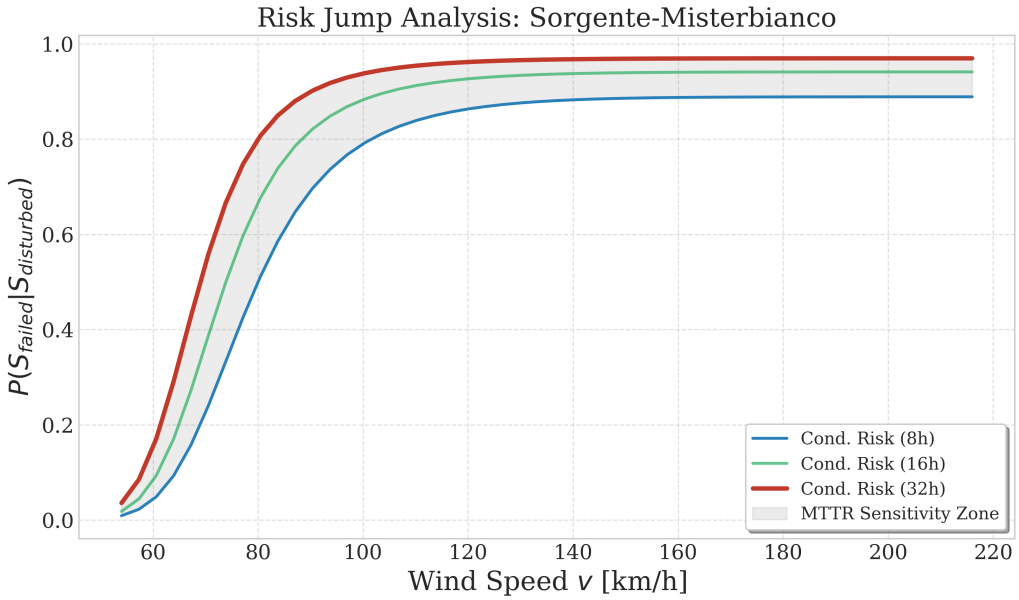

Figure 6.7: Risk jump analysis for the Sorgente-Misterbianco line.

The Risk Profile for the Sorgente-Misterbianco asset shows a little vulnerability to the restoration timeframe. The sensitivity zone illustrated in the MTTR Scenarios shows a wide range in the Conditional Probability of Failure, which indicates the likelihood of the 220 kV link transitioning from a transient grid disturbance to a permanent outage is very sensitive to how quickly maintenance response can be completed. This gap clearly illustrates that operational strategies such as rapid fault localization are as important to line health as hardening the infrastructure.

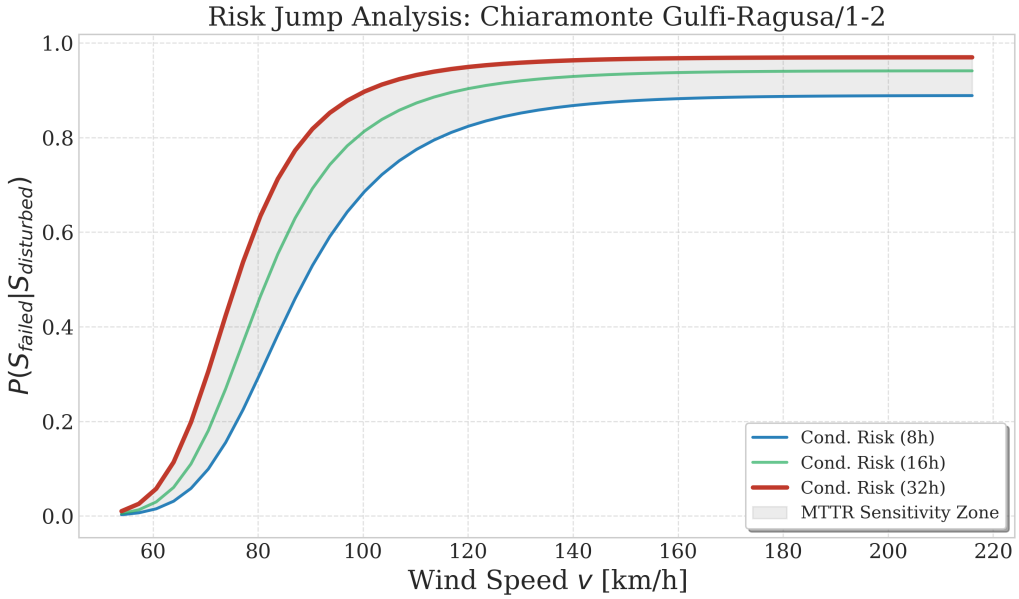

Figure 6.8: Risk jump analysis for the Chiaramonte Gulfi-Ragusa 1-2 line.

Unlike the Chiaramonte Gulfi-Ragusa link, the conditional risk of the Chiaramonte Gulfi-Ragusa link appears to evolve under more orderly conditions. A shallower slope of the probability curves indicates an increased inherent structural resistance to damage due to wind loads. As a result, a smaller region of sensitivity demonstrates that the system's failure probability is mostly confined, regardless of whether the restoration phase is delayed moderately. This illustrates a sufficient "buffer" to absorb variability in repair logistics without catastrophic spread of failure.

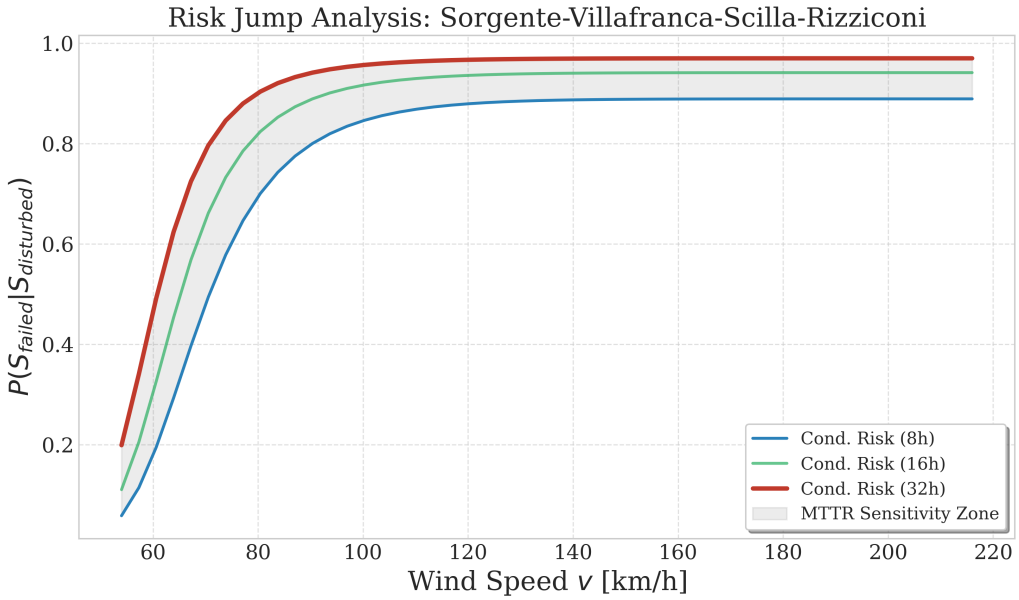

Figure 6.9: Risk jump analysis for the Sorgente-Villafranca-Scilla-Rizziconi line.

The Sorgente-Villafranca interconnector exhibits the largest increase in failure risk due to the highest rate of growth in its failure probability that has been documented for any of the systems examined. Due to this rapid failure probability rise at or near critical wind speed values, it will be necessary to implement emergency procedures with an exceptionally high degree of urgency since the operational safety margin is extremely small when experiencing peak-stress conditions.

Comparative Analysis

The variability in risk associated with the different assets are primarily due to the relationship between localized weather-related stress and the Bayesian calibrated fragility model.

Table 6.7: Comparison of sensitivity and fragility thresholds (in km/h) for the three lines.

Line Name	**Voltage**	**V50 [km/h]**	**Sensitivity**
Sorgente-Misterbianco	220 kV	95.0	Moderate
Chiaramonte Gulfi-Ragusa	220 kV	105.0	Low
Sorgente-Villafranca	380 kV	90.1	High

These results provide an understanding of the empirical factors that contribute to this difference:

- The Sorgente-Villafranca line exhibits a steeper transition from the operating state to the failure state compared with the two 220 kV lines due to the Bayesian calibration process that utilized the historical extreme wind data associated with each area in order to estimate the possible failure states for each transmission line; as a result, the sensitivity zone width for the Sorgente-Villafranca line is less than the sensitivity zones for the two 220 kV lines, which have a wider range of possible failure states.

- Asymptotic Behavior: The simulation data illustrates that the failure probability will converge to a limit strictly less than one. This behavior is due to the structure of the generator matrix Q, which includes both the failure rate λ and the restoration rate μ as the elements of the transition intensity matrix Q. The governing differential equation, $\frac{d\pi(t)}{dt} = \pi(t)Q$, also restricts the system from proceeding towards a total failure state. Therefore, as $t \to \infty$, the state probability vector $\pi(t)$ will eventually reach a steady-state distribution $\pi(\infty)$, and that steady-state distribution can be found by solving $\pi(\infty)Q = 0$. From this equation, we find the probability of being in the failed state S_3 at the steady-state time point to be given by:

$$\pi_3 = \frac{\lambda_{eff}}{\lambda_{eff} + \mu} \tag{6.6}$$

  Since the restoration strategy parameter $\mu > 0$, then the system will always transition back into the operational states S_1 or S_2, thus the probability π_3 will never equal one [66]. Therefore, this asymptotic value provides a basis to compare the performance of different systems with respect to their ability to limit damage caused by environmental stressors λ, regardless of the specific environmental stressors acting on each corridor.

Chapter 7

Conclusions and Future Work

7.1 Conclusions

This thesis presents a complete method for assessing the safe operation of high voltage double circuit transmission lines through a probability based model using a dynamic approach rather than a deterministic approach; thereby, moving from traditional deterministic criteria for evaluating the security of double circuit lines to an assessment of corridor level health status under extreme wind conditions by incorporating empirical incident data within the calibration of site specific fragility curves, which are integrated into a continuous time Markov process with multiple states.

These results illustrate that double circuit corridors are not solely dependent upon the mechanical structural capacity of the line, but also upon the efficiency of restoration logistics. The critical degraded state of the line occurs when the redundant capability of the double circuit line is exhausted, and restoration logistics play a significant role in determining the overall safety of the corridor. As stated in the introductory section of this study, while double circuits provide additional capacity to support increased load demands, they create structural dependencies among the circuits—particularly common cause failures—that were previously underestimated by deterministic models. Furthermore, the analysis of the Sicilian network demonstrates that the longer it takes to restore power, the greater the likelihood of catastrophic failure occurring when maintenance thresholds are exceeded. Moreover, this study bridges the gap between the static variables utilized in the traditional VAFFEL methodology and the dynamic nature of extreme weather events. The proposed framework dynamically updates transition rates based on current environmental conditions; thus, enabling grid managers to shift their reactive posturing to proactive posture. Lastly, a critical conclusion drawn from this research is that, relative to the optimization of restoration logistics, physical asset hardening provides diminishing returns. Therefore, for Transmission System Operators in storm prone areas, the most cost effective way to enhance grid resilience would be to intelligently allocate resources towards the expedited detection of faults and the reduction of mean time to repair (MTTR).

7.2 Research Limitations and Future Work

Although the VAFFEL-Markov framework offers a solid base to assess grid vulnerability in a quantitative manner, its current formulation has several restrictions and potential areas for future study. The most significant limitation is related to the use of a common cause failure rate, represented by a single coupled vulnerability constant, which does not necessarily reflect all of the spatially distributed, complex interdependencies of cascading failures across a larger regional grid. Another area for improvement in the synthetic incident generation process is that it assumes a uniform response to extreme stress conditions and therefore does not take into consideration secondary degradation mechanisms (i.e., icing or local mechanical fatigue).

There are at least three strategic research directions for future development to address the limitations of the current methodology. Firstly, the resolution of the meteorological input to the models needs to be improved, since the current modeling uses general benchmark values to represent extreme weather conditions and may not adequately capture the localized wind gusts present in specific locations. High-resolution meteorological data with spatio-temporal correlation information regarding wind field stresses will need to be used to capture the non-uniform stress distributions of long-span corridors and transition from a generalized exposure model to a site-specific risk assessment model. Secondly, the framework must consider the impact of power flow on failure events, because it currently considers failure events independently of the grid topology. Therefore, future versions of this framework should include both static and dynamic analyses of power flow after an N-1 contingency occurs in order to assess whether structural failure results in thermal overload on parallel circuitry and to improve the definition of the failure state S3. Thirdly, the advanced modeling should expand the Markovian engine to consider higher order state transitions that can account for latent failure states and permit the incorporation of real-time monitoring data from smart-grid sensor systems. In addition, incorporating economic implications of risk-informed maintenance decisions into the analysis, including the trade-off between preventive investments and curative operating expenses, will provide a more complete decision-making platform for long-term hardening of the grid.

Appendix: Technical Derivations and Parameter Calibration

1 Structural Limit Velocities (V_{ULS}) Derivation

The structural limit velocity V_{ULS} is obtained from the condition that the structural capacity (R_d) equals the design wind load (L_d).

1.1 Mechanical Equilibrium Condition

When the total resisting force (R_d) balances the cumulative aerodynamic pressure acting along the height of the tower (H):

$$R_d = \int_0^H \frac{1}{2}\rho \cdot v(z)^2 \cdot C_d \cdot D(z)\, dz \tag{1}$$

where $v(z)$ denotes the vertical wind speed profile and $D(z)$ the structure width at the given height z. To simplify this expression for design purposes, we define an Effective Projected Area $A_{eff} = \int_0^H D(z)\, dz$. Using the peak wind speed at the top of the tower as V_{ULS}, we can write the simplified static equilibrium equation:

$$R_d = \frac{1}{2}\rho \cdot V_{ULS}^2 \cdot C_d \cdot A_{eff} \tag{2}$$

This provides a direct relationship between the structural capacity (R_d) and the structural limit velocity (V_{ULS}). Solving this relationship for the structural limit velocity (V_{ULS}), expressed in km/h, gives us:

$$V_{ULS} = 3.6 \cdot \sqrt{\frac{2 \cdot R_d}{\rho \cdot C_d \cdot A_{eff}}} \tag{3}$$

1.2 Analytical Basis for Structural Parameters

We calculate the value of V_{ULS} based upon the structural features of the Sicilian grid assets, according to international standards [60, 67, 68]:

- **Yield strength of Steel (f_y):** For secondary lattice bracing of 220 kV towers, we use $235\, MPa$ (S235 steel); for primary leg reinforcement of 380 kV towers, we use $355\, MPa$ (S355 steel) [67].

- **Effective Area (A_{eff}):** Based on a solidity ratio of $\phi \approx 0.30$ applied to the overall silhouette of the tower, giving $18.5\,m^2$ for 220 kV towers and $24.2\,m^2$ for 380 kV towers [68].
- **Resistance Capacity (R_d):** Total load-bearing capability defined through the integration of f_y over the effective cross-sectional area of the steel members ($R_d \approx f_y \cdot A_{steel}$), which results in $12,500\,N$ and $16,500\,N$ for 220 kV and 380 kV towers, respectively [60].

1.3 Failure Probability Calibration (P_f)

The structural limit velocities established above (summarized in Tab. **??**) represent the saturation levels of the fragility model. Thus, as wind speed v approaches V_{ULS}, the failure probability P_f will converge to one:

$$\lim_{v \to V_{ULS}} P_f(v) \to 1.0 \tag{4}$$

Table 1: Historical failure events recorded between 2012 and 2020 (Wind speed in km/h).

Date	**Transmission Line**	**Voltage (kV)**	**Cause**	**Wind (km/h)**
2013-12-26	Corriolo - Caracoli/Sorgente	220	Strong Wind	82.76
2015-10-14	Corriolo - Caracoli/Sorgente	220	Strong Wind	88.49
2012-11-11	Corriolo - Caracoli/Sorgente	220	Strong Wind	86.08
2015-03-16	Corriolo - Caracoli/Sorgente	220	Strong Wind	88.13
2014-11-05	Corriolo - Caracoli/Sorgente	220	Strong Wind	83.74
2013-02-11	Corriolo - Caracoli/Sorgente	220	Strong Wind	82.87
2015-01-30	Corriolo - Caracoli/Sorgente	220	Strong Wind	90.04
2019-04-22	Corriolo - Caracoli/Sorgente	220	Strong Wind	91.01
2018-03-01	Corriolo - Caracoli/Sorgente	220	Strong Wind	89.78
2019-12-04	Melilli-Ragusa/1-2	220	Strong Wind	69.70
2012-12-02	Melilli-Ragusa/1-2	220	Strong Wind	69.88
2012-12-03	Melilli-Ragusa/1-2	220	Strong Wind	70.85
2020-09-14	Melilli-Ragusa/1-2	220	Other	N/A
2012-07-04	Melilli-Ragusa/1-2	220	Other	N/A
2018-04-01	Misterbianco-Melilli/1-2	220	Strong Wind	68.26
2013-06-02	Misterbianco-Melilli/1-2	220	Strong Wind	66.71
2015-12-23	Misterbianco-Melilli/1-2	220	Other	N/A
2018-01-18	Sorgente-Misterbianco	220	Strong Wind	100.98
2012-05-17	Sorgente-Misterbianco	220	Strong Wind	88.16
2018-03-07	Sorgente-Misterbianco	220	Strong Wind	93.49
2013-05-16	Sorgente-Misterbianco	220	Strong Wind	96.95
2015-01-30	Sorgente-Misterbianco	220	Strong Wind	109.01
2018-03-31	Sorgente-Misterbianco	220	Strong Wind	104.29
2018-01-03	Sorgente-Misterbianco	220	Strong Wind	112.75
2020-02-04	Sorgente-Misterbianco	220	Strong Wind	97.49
2012-01-06	Sorgente-Misterbianco	220	Strong Wind	116.60
2018-03-31	Sorgente-Misterbianco	220	Strong Wind	107.50
2012-01-07	Sorgente-Misterbianco	220	Strong Wind	113.00
2017-05-11	Sorgente-Misterbianco	220	Strong Wind	87.73
2018-03-01	Sorgente-Misterbianco	220	Strong Wind	95.87
2020-12-28	Sorgente-Misterbianco	220	Strong Wind	89.71
2018-02-13	Sorgente-Misterbianco	220	Strong Wind	87.95
2019-04-21	Sorgente-Misterbianco	220	Strong Wind	103.36
2018-12-09	Sorgente-Misterbianco	220	Strong Wind	111.06
2018-01-18	Sorgente-Misterbianco	220	Strong Wind	111.82
2013-03-21	Sorgente-Misterbianco	220	Strong Wind	92.38
2012-07-22	Sorgente-Misterbianco	220	Other	N/A
2014-05-20	Sorgente-Misterbianco	220	Other	N/A
2014-02-03	Sorgente-Misterbianco	220	Other	N/A
2013-05-03	Sorgente-Misterbianco	220	Other	N/A
2014-04-04	Sorgente-Villafranca-Scilla-Rizziconi	380	Strong Wind	90.07

Bibliography

[1] Terna S.p.A. *Codice di Rete per la Trasmissione, il Dispacciamento, lo Sviluppo e la Sicurezza della Rete*. Including Annex A.21 on Wildfire procedures and Annex A.72 on Resilience Guidelines. Terna S.p.A. 2024. URL: https://www.terna.it/it/sistema-elettrico/codice-rete/allegati (cit. on p. 3).

[2] Enrico Maria Carlini, Salvatore Favuzza, S. E. Giangreco, Fabio Massaro, and Cristiano Quaciari. "Uprating an overhead line. Italian TSO applications to increase system N1 security". In: *Proceedings of the IEEE International Conference on Renewable Energy Research and Applications (ICRERA)*. Oct. 2013. DOI: 10.1109/ICRERA.2013.6749875 (cit. on p. 3).

[3] Mattia Boiani, Luca Buono, Franco Di Bona, Gaia Leone, and Francesco Palone. "Electrical Parameters of the New "5-Phases" Overhead Lines". In: *AEIT* (2024). DOI: 10.23919/aeit63317.2024.10736790 (cit. on p. 3).

[4] Luca Rusalen and Roberto Benato. "Multiconductor Power Flow of HV/EHV Italian Network". In: *AEIT* (2024). DOI: 10.23919/aeit63317.2024.10736870 (cit. on pp. 3, 8, 9).

[5] M. G. Ippolito, F. Massaro, and C. Cassaro. "HTLS Conductors: A Way to Optimize RES Generation and to Improve the Competitiveness of the Electrical Market—A Case Study in Sicily". In: *Journal of Electrical and Computer Engineering* (2018). URL: https://iris.unipa.it/retrieve/handle/10447/302236/599981/paper%20JECE%20pubblicato.pdf (cit. on p. 3).

[6] Terna S.p.A. *2023 Development Plan: The Hypergrid project and development requirements*. Tech. rep. Strategic planning for Italian National Transmission Grid. Terna S.p.A., 2023. URL: https://download.terna.it/terna/2023_Hypergrid_project_and_development_requirements_8db79602cedc732.pdf (cit. on p. 4).

[7] Terna S.p.A. *Allegato A.15: Sistemi di Protezione della Rete di Trasmissione Nazionale*. Technical specification for protection and control systems. Terna S.p.A. 2022. URL: https://www.terna.it/en/electric-system/grid-codes (cit. on p. 5).

[8] Red Eléctrica de España. *Plan de Desarrollo de la Red de Transporte de Energía Eléctrica 2021-2026*. Tech. rep. Official Spanish Grid Development Plan. REDEIA, 2024. URL: https://www.ree.es/es/actividades/planificacion-de-la-red (cit. on p. 6).

[9] Red Eléctrica de España. *Especificaciones Técnicas para Líneas de Transporte de Alta Tensión*. Standardized technical specifications for 400kV and 220kV lines. Redeia. 2024 (cit. on pp. 6, 8).

[10] Red Eléctrica de España. *IT-01: Criterios de diseño para líneas de transporte de 400 kV*. Internal technical instruction for the design and construction of 400 kV overhead transmission lines. Redeia. Alcobendas, Spain, 2022. URL: https://www.ree.es/es/proveedores/documentacion-tecnica/instrucciones-tecnicas (cit. on p. 8).

[11] Red Eléctrica de España. *P.O. 11.1: Sistemas de protección de las redes de transporte*. Spanish Grid Operating Procedure for Protection Systems. Redeia. 2023 (cit. on p. 8).

[12] Red Eléctrica de España. *P.O. 12.2: Instalaciones de comunicaciones y teleprotección*. Spanish Grid Operating Procedure for Communications. Redeia. 2023 (cit. on p. 8).

[13] Réseau de Transport d'Électricité (RTE). *Schéma de Développement du Réseau de Transport d'Électricité (SDR)*. Tech. rep. Strategic 10-year grid development plan. RTE France, 2024. URL: https://www.rte-france.com/analyses-tendances-et-prospectives/le-schema-decennal-de-developpement-du-reseau (cit. on pp. 9, 11).

[14] Réseau de Transport d'Électricité (RTE). *Conception et Maintenance des Lignes Aériennes HT/THT*. Standardized technical requirements for EHV/HV overhead lines. RTE France. 2024 (cit. on pp. 9, 11).

[15] Réseau de Transport d'Électricité (RTE). *Adaptation du Réseau au Changement Climatique et Résilience des Infrastructures*. Tech. rep. Technical report on grid resilience and climate adaptation. RTE France, 2024 (cit. on pp. 9–11).

[16] Amprion and 50Hertz and TenneT and TransnetBW. *Netzentwicklungsplan Strom 2037/2045 (2023)*. Tech. rep. Official German Grid Development Plan. Transmission System Operators (TSOs), 2024. URL: https://www.netzentwicklungsplan.de (cit. on pp. 12, 14).

[17] VDE Verband der Elektrotechnik. *VDE-AR-N 4120: Technische Anschlussregeln Hochspannung*. Technical rules for EHV grid connection. VDE Verlag. 2024 (cit. on pp. 12, 14).

[18] Amprion GmbH. *Resilienz der Übertragungsnetze im Kontext der Energiewende*. Tech. rep. Technical report on grid resilience and system recovery. Amprion, 2024 (cit. on p. 13).

[19] Statnett SF. *Nettutviklingsplan (Network Development Plan) 2024*. Tech. rep. Strategic grid expansion plan for Norway. Statnett, 2024. URL: https://www.statnett.no/en/about-statnett/publications/network-development-plan-2024 (cit. on pp. 15, 17).

[20] Statnett SF. *Design Basis for High-Voltage Overhead Lines in Norway*. Technical standards for structural and electrical design in sub-arctic conditions. Statnett. 2024 (cit. on pp. 15, 17).

[21] Statnett SF. *System Reliability and Resilience in Extreme Climates*. Tech. rep. Technical report on grid performance and maritime maintenance strategies. Statnett, 2024 (cit. on pp. 16, 17).

[22] Swissgrid Ltd. *Strategic Grid 2025/2030: Expanding the Swiss Transmission System*. Tech. rep. Comprehensive network expansion plan for Switzerland. Swissgrid, 2024. URL: https://www.swissgrid.ch/en/home/operation/grid-data/grid-development.html (cit. on pp. 18, 19).

[23] Swissgrid Ltd. *Technical Standards for EHV Underground and Overhead Infrastructure*. Standardized engineering requirements for mixed-media corridors. Swissgrid. 2024 (cit. on pp. 18, 19).

[24] Swissgrid Ltd. *Grid Resilience and Maintenance Strategies in Alpine Topographies*. Tech. rep. Technical report on pylon design and system recovery in mountain regions. Swissgrid, 2024 (cit. on p. 19).

[25] National Grid ESO. *Offshore Transmission Network Review: Final Recommendations and Implementation*. Tech. rep. Strategic review of UK offshore grid integration. National Grid, 2024. URL: https://www.nationalgrideso.com/document/276701/download (cit. on pp. 20, 22).

[26] National Grid Electricity Transmission. *The T-Pylon: Engineering and Design Specifications for 400 kV Monopoles*. Technical design basis for innovative monopole transmission. National Grid. 2024 (cit. on pp. 20, 22).

[27] National Grid Electricity Transmission. *Grid Resilience and Asset Management in Maritime Climates*. Tech. rep. Technical report on infrastructure reliability and recovery strategies. NGET, 2024 (cit. on pp. 20, 22).

[28] European Commission. "Regulation (EU) 2017/1485 establishing a guideline on electricity transmission system operation (SOGL)". In: *Official Journal of the European Union* L 220 (2017) (cit. on p. 24).

[29] ENTSO-E. *Methodology for Coordinating Operational Security Analysis (CSAM)*. Technical Methodology. European Network of Transmission System Operators for Electricity, 2021 (cit. on p. 24).

[30] ACER. *Decision No 07/2024 on the Amendment of the Methodology for Coordinating Operational Security Analysis*. Tech. rep. Annex I: Second CSAM Amendment. European Union Agency for the Cooperation of Energy Regulators, 2024. URL: https://www.creos-net.lu/fileadmin/dokumente/codes_reseaux/ACER_N_07-2024.pdf (cit. on p. 24).

[31] *CEI EN 50341-1: Overhead electrical lines exceeding AC 1 kV - Part 1: General requirements*. Milano, Italia: Comitato Elettrotecnico Italiano, 2012 (cit. on p. 24).

[32] Terna S.p.A. *Piano di Sviluppo 2023 - Overview*. Tech. rep. Terna S.p.A., 2023. URL: https://download.terna.it/terna/Terna_Piano_Sviluppo_2023_Overview_8db25484d720abe.pdf (cit. on p. 26).

[33] Terna S.p.A. *Documento Metodologico per l'applicazione dell'analisi costi benefici applicata al Piano di Sviluppo 2023*. Tech. rep. Terna S.p.A., 2023. URL: https://download.terna.it/terna/Terna_Piano_Sviluppo_2023_Documento_Metodologico_applicazione_analisi_costi_benefici_8db254c3b3edff1.pdf (cit. on p. 26).

[34] Terna S.p.A. *Innovation for a robust and resilient grid*. 2023. URL: https://www.terna.it/en/sustainability/innovation-robust-resilient-grid (cit. on p. 26).

[35] Terna S.p.A. *Pianificazione della Rete Elettrica*. Tech. rep. Terna S.p.A., 2023. URL: https://download.terna.it/terna/Terna_Piano_Sviluppo_2023_Pianificazione_Rete_Elettrica_8db25486f9b1334.pdf (cit. on p. 26).

[36] Secretaría de Estado de Energía. *Procedimiento de Operación 1.1: Criterios de funcionamiento y seguridad para la operación del sistema eléctrico*. Resolution of April 5, 2016. Boletín Oficial del Estado (BOE). 2016. URL: https://www.cnmc.es/sites/default/files/editor_contenidos/Energia/Normativa_M_Electrico/P.O.%201.1%20Criterios%20de%20funcionamiento%20y%20seguridad%20para%20la%20operaci%C3%B3n%20del%20sistema%20el%C3%A9ctrico%20%282%29.pdf (cit. on p. 27).

[37] Red Eléctrica de España. *Negocio Eléctrico en España*. Accessed March 2026. 2025. URL: https://www.ree.es (cit. on pp. 27, 28).

[38] Antón García, Albert Riera, Alberto Martín, João Peças Lopes, Francisco Fernandes, and Rui Sousa. *Analysis of events leading to the peninsular blackout of April 28, 2025*. Tech. rep. Compass Lexecon and INESC TEC, July 2025. URL: https://aelec.es/wp-content/uploads/2025/07/20250730_CL_INESCTEC_Blackout_full-report_en.pdf (cit. on p. 27).

[39] RTE. *Bilan de la sûreté du système électrique français en 2024*. Tech. rep. Réseau de Transport d'Électricité, Sept. 2024. URL: https://assets.rte-france.com/prod/public/2025-09/2025-09-16-bilan-surete-2024.pdf (cit. on pp. 29, 30).

[40] RTE. *Schéma Décennal de Développement du Réseau (SDDR) 2025*. Tech. rep. Réseau de Transport d'Électricité, Feb. 2025. URL: https://assets.rte-france.com/prod/public/2025-02/RTE_SDDR2025_Synthese.pdf (cit. on pp. 29, 30).

[41] CRE. *Public consultation No. 2025-08 on the ten-year development plan for the RTE network drawn up in 2025*. Tech. rep. Commission de Régulation de l'Énergie, Sept. 2025. URL: https://www.cre.fr/fileadmin/Documents/Consultations_publiques/2025/250918_Consultation_2025-08_SDDR_RTE-en.pdf (cit. on p. 30).

[42] RTE. *Bilan prévisionnel 2025 - Résumé exécutif et synthèse*. Tech. rep. Réseau de Transport d'Électricité, Dec. 2025. URL: https://assets.rte-france.com/prod/public/2025-12/2025-12-09-BP2025-resume-executif-synthese.pdf (cit. on p. 30).

[43] VDE FNN. *VDE-AR-N 4130: Technical Connection Rules for Extra-High Voltage (TAR Extra-High Voltage)*. Nationally uniform requirements for installations connected to the $\geq$ 220 kV grid. 2025 (cit. on pp. 31, 32).

[44] 50Hertz, Amprion, TenneT, and TransnetBW. *Netzentwicklungsplan Strom 2037/2045, Version 2025, 1. Entwurf*. Tech. rep. German Transmission System Operators, 2025. URL: https://www.netzentwicklungsplan.de (cit. on pp. 31, 32).

[45] Amprion GmbH. *Amprion Connects: Factbook September 2025*. Tech. rep. Amprion Investor Relations, 2025 (cit. on pp. 31, 32).

[46] VDE FNN. *Technical connection rules (TCR) for connecting electrical equipment to the grid*. General framework for renewable energy integration and grid security. 2026 (cit. on pp. 31, 32).

[47] VDE FNN. *VDE-AR-N 4210-5: Witterungsabhängiger Freileitungsbetrieb (WAFB)*. Application rule for weather-related overhead line operation. 2021 (cit. on p. 32).

[48] Gerd Kjølle and Arnt Ove Eggen. *FASIT: 30 years of data on faults and interruptions for the entire Norwegian power system*. SINTEF Blog. Jan. 2026. URL: https://blog.sintef.com (cit. on p. 33).

[49] M. Rekinger, M. Hofmann, A. Chaouachi, E. Karangelos, L. Wehenkel, and G. H. Kjølle. *A transition roadmap towards probabilistic reliability management*. Tech. rep. The GARPUR Project, Oct. 2017. URL: http://www.garpur-project.eu (cit. on p. 33).

[50] Ø. R. Solheim, T. Trötscher, and G. H. Kjølle. "Wind dependent failure rates for overhead transmission lines using reanalysis data and a Bayesian updating scheme". In: *2016 International Conference on Probabilistic Methods Applied to Power Systems (PMAPS)*. Beijing, 2016. DOI: 10.1109/PMAPS.2016.7764104 (cit. on p. 34).

[51] *Biennial Progress Report on Operational Probabilistic Coordinated Security Assessment and Risk Management*. Tech. rep. European Network of Transmission System Operators for Electricity (ENTSO-E), Dec. 2023. URL: https://www.entsoe.eu (cit. on p. 34).

[52] Øystein Rognes Solheim, Ingeborg Ligaarden, Boye Høverstad, Thomas Trötscher, Markus Andersen, and Magnus Korpås. "Vaffel - a tool for forecasting transmission line failures based on Bayesian updating, renalysis data and medium range weather forecasts". In: June 2024, pp. 1–6. DOI: 10.1109/PMAPS61648.2024.10667068 (cit. on pp. 38, 61).

[53] Researcher Name. "Bayesian Updating of Failure Rates in Transmission Networks". In: *Grid Security and Resilience* (2022). Methodological reference for Bayesian failure rate estimation (cit. on pp. 38, 62).

[54] Jovan Nahman and Dušan Mijušković. "Reliability analysis of high voltage transmission lines". In: *Electric Power Systems Research* 16.1 (1989), pp. 75–80 (cit. on pp. 43, 44).

[55] Roy Billinton and Ronald N Allan. *Reliability Evaluation of Power Systems*. Springer Science & Business Media, 1992 (cit. on pp. 43–45).

[56] *IEEE Recommended Practice for the Design of Reliable Industrial and Commercial Power Systems*. IEEE, 2007 (cit. on pp. 43, 67).

[57] CIGRE Working Group B2.31. *Guide to the selection of weather parameters for overhead lines*. Tech. rep. Technical Brochure 299. Paris, France: CIGRE, 2006 (cit. on p. 57).

[58] Statnett. *Faults in the main grid 2019: Annual report on faults and outages*. Tech. rep. Statnett SF, 2020 (cit. on p. 57).

[59] S. Quassia et al. "Probabilistic Assessment of Wind-Induced Risks in Mediterranean Power Systems". In: *Reliability Engineering System Safety* 174 (2018), pp. 102–115 (cit. on p. 57).

[60] Comitato Elettrotecnico Italiano. *CEI EN 50341-1: Linee elettriche aeree con tensione superiore a 1 kV CA. Parte 1: Prescrizioni generali - Specifiche comuni*. Standard. Milano, Italia: CEI, 2012 (cit. on pp. 61, 80, 81).

[61] Energiforsk. *High Voltage Equipment Reliability Data*. Tech. rep. 2023:974. Accessed: 2026-03-07. Energiforsk, 2023. URL: https://energiforsk.se/media/32998/2023-974-high-voltage-equipment-reliability-data.pdf (cit. on p. 62).

[62] Marvin Rausand and Mary Ann Lundteigen. *Reliability of Safety-Critical Systems: Theory and Applications*. John Wiley & Sons, 2014. DOI: 10.1002/9781118776353 (cit. on p. 67).

[63] CIGRE Working Group B2.17. *Reliability of Transmission Lines*. Tech. rep. 353. CIGRE, 2008 (cit. on p. 68).

[64] Terna S.p.A. *Codice di Rete, Capitolo 10 – Salvaguardia della sicurezza*. Applicabile a partire dal 1° gennaio 2025 in relazione all'implementazione del TIDE. Terna - Gestore della Rete Trasmissione Nazionale. 2025. URL: https://www.terna.it/it/sistema-elettrico/codice-rete (cit. on p. 70).

[65] Commissione Europea. *Regolamento (UE) 2017/1485 della Commissione del 2 agosto 2017 che stabilisce orientamenti in materia di gestione del sistema di trasmissione dell'energia elettrica*. Tech. rep. L 220/1. Testo rilevante ai fini del SEE. Gazzetta ufficiale dell'Unione europea, 2017. URL: https://eur-lex.europa.eu/legal-content/IT/TXT/?uri=CELEX:32017R1485 (cit. on p. 70).

[66] Sheldon M. Ross. *Introduction to Probability Models*. 11th. Chapter 6: Continuous-Time Markov Chains; Section 6.4: The Limiting Probabilities. Academic Press, 2014. ISBN: 978-0124079489 (cit. on p. 76).

[67] UNI. *Hot rolled structural steels - Part 2: Technical delivery conditions for non-alloy structural steels*. Standard for S235 and S355 steel grade specifications. Ente Nazionale Italiano di Unificazione, 2005 (cit. on p. 80).

[68] IEC. *Design criteria of overhead transmission lines*. Standard for wind load application and solidity ratio definitions. International Electrotechnical Commission, 2017 (cit. on pp. 80, 81).

Dedications

Vorrei dedicare questa tesi a mio nonno, che mi ha aiutato per tutta la carriera accademica e ha sempre voluto che finissi questo percorso. Purtroppo sei mancato prima e non potrai leggerla però mi ricorderò sempre che ci sei stato quando serviva.
Ai i miei genitori per il supporto costante da casa e a mio fratello Giordano per avere creduto che prima o poi ce l'avrei fatta.
A Ernesta che mi è stata sempre vicino dall'inizio di questa magistrale e con cui ho affrontato così tanti esami che non sembra vero avercela fatta.
A Davide per essermi stato sempre vicino anche dalla lontana Colonnella.
A Satti per tutte le ore passate insieme su Discord e per la compagnia di cui avevo bisogno alla fine del percorso.
A Cecilia per essere arrivata nella mia quotidianità e dato leggerezza alle mie giornate.
A tutti i miei ex-compagni di corso che mi hanno ispirato a farcela quando la laurea sembrava così lontana.